Exploring the mechanisms underlying the phenotype of MCAD deficiency with Systems Medicine

Martines, Anne-Claire

Chapter 4

The role of hepatic fatty-acid oxidation during cold stress: remodeling of hepatic metabolism in a mouse with medium-chain acyl-CoA dehydrogenase deficiency

A.M.F. Martines[1,#], Wenxuan Zhang[1,2,#], Albert Gerding[1,3], Maaike Goris[4], Marcel de Vries[1], Mirjam H. Koster[1,4], Laura Bongiovanni[5], Alain de Bruin[1,5], Rob H. Henning[4], Terry G. J. Derks[1,6], Rainer Bischoff[2], Dirk-Jan Reijngoud[1,2], Barbara M. Bakker[1,*]

[#]Authors contributed equally to this work.

[1] Laboratory of Pediatrics, Center of Liver, Digestive and Metabolic Diseases, University of Groningen, Groningen, University Medical Center Groningen, Groningen, The Netherlands,
[2] Department of Analytical Biochemistry, University of Groningen, Groningen, The Netherlands
[3] Department of Laboratory Medicine, University of Groningen, University Medical Center Groningen, The Netherlands
[4] Department of Anesthesiology, University of Groningen, University Medical Center Groningen, Groningen, The Netherlands
[5] Department of Pathobiology, Faculty of Veterinary Medicine, Dutch Molecular Pathology Center, Utrecht University, The Netherlands
[6] Section of Metabolic Diseases, Beatrix Children's Hospital, University Medical Center of Groningen, University of Groningen.

Journal publication in preparation

Abstract

Children with a deficiency in the mitochondrial fatty-acid β-oxidation (mFAO) enzyme medium-chain acyl-Coenzyme A dehydrogenase (MCAD) are at risk of life-threatening low blood glucose levels. To elucidate the role of liver MCAD in the response to energetic stress, fasted MCAD-deficient (MCAD-KO) and wild-type (WT) mice were exposed to cold. MCAD-KO mice showed lower blood glucose levels and hepatic amino acid levels, and higher liver weights, liver triglycerides and blood medium-chain acyl-carnitine levels. Detailed lipidomics analysis revealed an accumulation of triglyceride species containing medium-chain fatty-acyl branches in the liver.

Our results are consistent with a key role of liver mFAO in glucose homeostasis during cold stress. MCAD-KO mice exhibit a compensatory response in which amino acids partly take over the role of fatty acids in the generation of ATP, glucose, and ketone bodies, while excess medium-chain fatty-acid intermediates are exported and rerouted into triglycerides.

Introduction

Hepatic mitochondrial fatty-acid beta-oxidation (mFAO) plays an important role in energy homeostasis during fasting and conditions of high energy demand. The pathway provides energy for *de novo* glucose production and substrate for ketone body production [1–3]. Consequently, individuals with a defect in mFAO often present with low blood glucose and ketone body concentrations (hypoketotic hypoglycemia) [1–3]. The most prevalent mFAO disorder is a complete deficiency of the enzyme medium-chain acyl-CoA dehydrogenase (MCAD). While MCAD-deficient (MCADD) children may tolerate overnight fasting [4,5], a combination of prolonged fasting and an additional trigger, such as (combinations of) fever, decreased gastrointestinal intake or increased losses, increases the risk of hypoketotic hypoglycemia and sudden-infant death [1,6–9].

To investigate the etiology of MCADD, an MCAD-deficient (MCAD-KO) mouse model has been generated [10,11]. The MCAD-KO mice exhibited the elevated blood medium-chain acyl-carnitines that are also characteristic of human MCADD, and an enhanced rate of neonatal death [10]. Just as MCADD children, MCAD-KO mice were quite resilient to fasting alone and maintain normal blood glucose levels during 24 hours of fasting [10,12]. However, a combination of fasting and cold exposure (4° C) was lethal or led to very low body temperatures in the KO, but not in the wild type (WT) mice [10]. Cold intolerance is a common feature of mFAO deficient mouse models and was also observed when either of the genes encoding short-, long-, or very-long-chain acyl-CoA dehydrogenase (SCAD, LCAD and VLCAD) were deleted (reviewed in [13]).

When mice are exposed to cold stress, brown adipose tissue (BAT) uses glucose, amino-acid, and fatty-acid catabolism for non-shivering thermogenesis [14–16]. Cold stress increases the expression of genes involved in fatty-acid uptake and mFAO in BAT [17]. In this condition, the liver plays a key role in the supply of substrate by increased gluconeogenesis [18] and acyl-carnitine production and secretion [19,20]. In line with this, the liver exhibits a higher expression of genes involved in mFAO and a lower expression of genes in fatty-acid synthesis [21–23]. When mFAO or fatty-acid uptake is defective, the BAT relies more heavily on glucose and amino acids. This leads to a higher requirement for *de novo* glucose production by the liver. Accordingly, fasting in combination with cold exposure resulted in lower blood glucose concentrations in VLCAD-KO compared to WT mice [24–26]. To date however, there are no reports on the liver function of MCAD-KO mouse during cold stress, nor of any other physiological parameters but rectal temperature [10,27]. Therefore, the aim of this study was to investigate liver function in MCAD-KO mice during combined cold exposure and fasting.

In this study, MCAD-KO mice were fasted for 14 h at 21 °C and subsequently for another 4-6 h at 4 °C. The phenotype of young mice (8 weeks) was more affected than that of adult mice (16-20 weeks). At the end of the challenge, the blood glucose concentration of young MCAD-KO mice was lower than that of their WT counterparts, while ketone-body levels were similar. Liver amino-acid levels were lower in MCAD-KO mice compared to WT, consistent with a higher substrate use for gluconeogenesis. Medium-chain acyl-carnitine levels (notably C10:1) were elevated in the blood of the KO mice, but unaffected in the liver. In-depth hepatic lipidomic analysis revealed accumulation of triglyceride (TG) species containing C6-C14 acyl chains, suggesting that medium-chain mFAO intermediates were rerouted into (partial) chain elongation and/or storage. This is the first time that the liver metabolism of the MCAD-KO mouse was studied under severe energetic stress. We conclude

that it is a valuable model to gain insight into metabolic adaptations in MCADD and provide further evidence for the crucial role of liver mFAO in protection against cold stress.

Results

Young MCAD-KO mice are more vulnerable to cold exposure than adult MCAD-KO mice.

To expose adult (16-20 weeks old) MCAD-KO mice to severe energetic stress, they were fasted for 14 hours and subsequently exposed to a 4°C environment, still in the absence of food. Cold exposure for 4-6 hours induced a substantial drop in the body temperature of 4 out of 8 fasted KO mice, while all 7 detected WT mice maintained a stable temperature (Figure 1A).

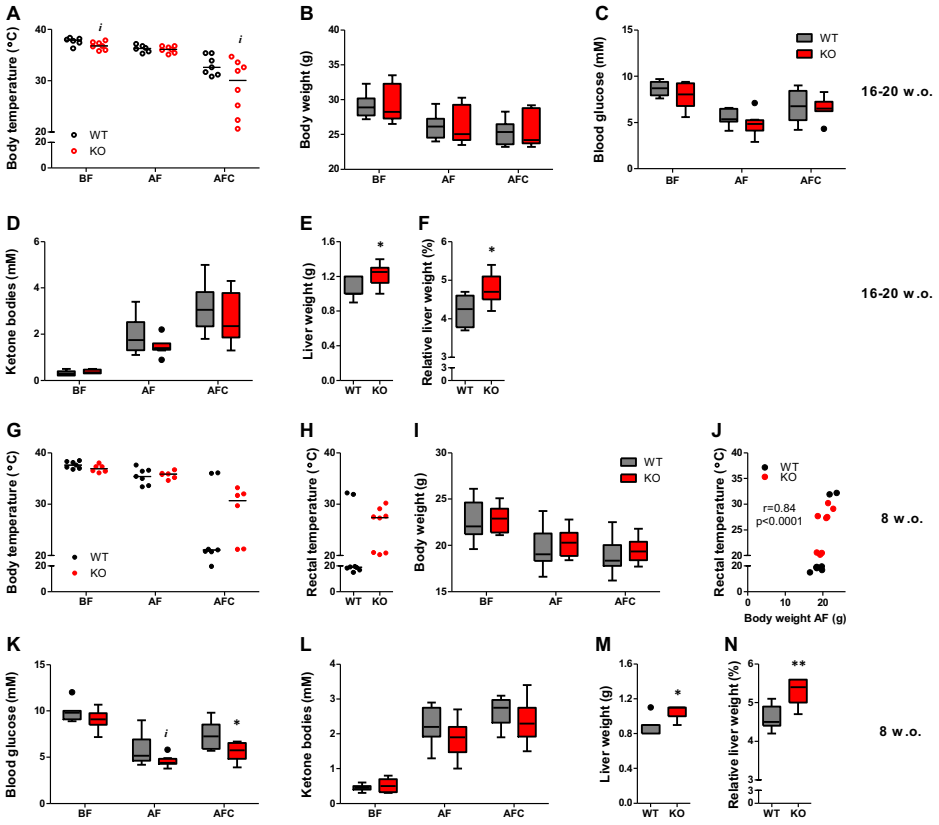

Figure 1. Biometric results of 8- and 16-20-weeks-old mice. Body temperature measured by intraperitoneally-implanted logger (**A,G**), body weight (**B,I**), blood glucose (**C,K**) and ketone bodies (**D,L**) before fasting (BF), after 14 hrs of fasting, before cold exposure (AF) and after fasting plus cold exposure (AFC), absolute liver weight (**E,M**) and relative liver weight (% of body weight) (**F,N**) of the 16-20 weeks-old (**A-F**) and 8 weeks-old mice (**G,I,K-N**) and rectal temperature (**H**), rectal temperature versus body weight after 14 hrs of fasting (**J**) of the 8- weeks-old mice. n=6-8 for both WT and KO. The results are represented as Tukey box and whisker plots, where the black-filled jagged circles indicate individual mice falling outside the 75% percentile plus 1.5·inter-quartile range (IQR) or 25% percentile minus 1.5·IQR. Indicative, *i*: p<0.1, *: p<0.05, **: p<0.01, ***: p<0.001 and ****: p<0.0001 compared to WT. All box plots and indications of significance in the remainder of this report are represented in the same way as this figure.

The variation in the MCAD-KO group was substantial, possibly because the start of the temperature decline was shifted in time between individuals (Supplementary figure S1A). The body weight decreased to a similar extent in both groups, and was similar in MCAD-KO and WT mice (Figure 1B). In addition, blood glucose and ketone-body concentrations were similar between WT and KO mice (Figure 1C-D). The absolute and relative liver weights were, however, significantly higher in MCAD-KO than WT mice at the end of the experiment (Figure 1E, F).

Previously, a significantly lower body temperature has been reported in 8-weeks old, fasted, cold-exposed MCAD-KO mice relative to their WT counterparts [10]. When we repeated the experiment in 8 weeks old mice, more animals showed a drop in body temperature, in this case also in the WT group (Supplementary figure S1B). This entailed, 33.3% (2/6) and 71% (5/7) of the KO and WT mice, respectively, of which the body temperature could be measured (Figure 1G,H; Supplementary figure S1B). No significant difference between the genotypes was observed (Figure 1G,H). Furthermore, the body weight decreased in both genotypes to a similar extent, and also here was similar MCAD-KO and WT mice (Figure 1I). A correlation analysis revealed that the animals with a lower body weight also had a lower body temperature after cold exposure (Figure 1J and Supplementary Figure S1C). Interestingly, after cold exposure the blood-glucose concentration was significantly lower in young MCAD-KO than in WT mice (Figure 1K), albeit without any effect on the level of ketone bodies (Figure 1L). Apparently, MCAD deficiency affects the blood glucose concentration only under severe energetic stress, i.e. upon a combination of fasting and cold stress in young animals. This is similar to the situation in patients, who also present with hypoglycemia only at a young age (typically 0-2 years), during overnight fasting in combination with another stress factor. Relative liver weights were significantly higher in young KO compared to the WT mice (Figure 1M,N), as observed for adult mice but the difference was even more pronounced in young mice. Altogether, based on the metabolic results, these results show that young MCAD-KO mice are more vulnerable to cold exposure than adult mice.

Higher plasma acyl-carnitines and NEFAs in fasted, cold-exposed MCAD-KO mice

Previously, significantly lower plasma alanine levels have been reported in fasted MCAD-KO compared to WT mice, while valine, leucine and isoleucine were similar [28]. We did not observe significant differences in amino acid concentrations between 8 weeks old MCAD-KO and WT mice, except for α-aminobutyric acid, which was lower in the MCAD-KO group (Figure 2A and Supplementary figure S2A). Elevated blood medium-chain acyl-carnitine levels are an important biomarker for MCAD deficiency [29–33]. Indeed, the C6- to C10-acyl-carnitine concentrations were higher in MCAD-KO compared to WT mice, under all conditions and in both age groups (Figure 2B-D and Supplementary figure S2B-S). In agreement with previous findings in MCAD-KO mice [10,28,34], particularly C10:1 was elevated. This is in contrast to human MCADD patients, in which C8-acyl-carnitine accumulates most [29–33]. The difference between MCAD-KO and WT was most pronounced after fasting, irrespective of cold exposure (Figure 2B-D, Supplementary figure S2B-S and Supplementary table ST1). Finally, plasma NEFA levels after cold exposure were significantly higher in the young MCAD-KO mice (Figure 2E). During cold stress enhanced triglyceride lipolysis by adipose tissue results in increased release of NEFAs [35].

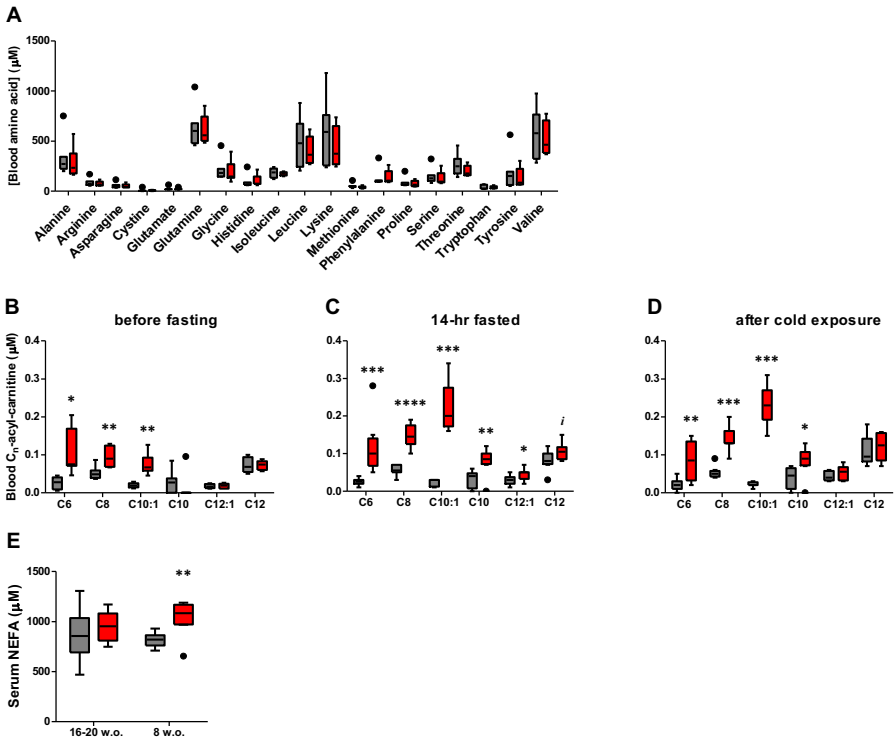

Figure 2. Blood metabolite concentrations. Plasma amino acid concentrations after cold exposure (**A**), blood acyl-carnitine concentrations (**B-D**) of the 8-weeks-old mice, and serum NEFA levels after cold exposure (**E**).

The difference in plasma NEFA levels may therefore either be due to the higher release of NEFAs by adipose tissue, or to the defective mFAO pathway in the liver, or a combination of both.

Altered amino-acid and lipid handling in the liver of cold-exposed MCAD-KO mice

Subsequently, we focused on metabolic adaptations in the liver of fasted, cold-exposed animals. Hepatic amino acids may serve as alternative substrates and fuels for ketogenesis and gluconeogenesis in the MCAD-KO mice. In line with this, we observed significantly lower amino-acid concentrations in livers of cold-exposed fasted MCAD-KO mice (Figure 3A, Supplementary figure 3A and Supplementary table ST1). The difference was again more pronounced in the young mice. In these mice, the levels were significantly lower for glutamine, glycine, leucine, lysine, serine, threonine, tyrosine and L-cystathionine and indicative (*i*, $p<0.1$) for alanine, glutamic acid, α-aminobutyric acid and ornithine. In the adult KO mice, only glycine levels were significantly lower, although the same trend was observed for other amino acids (Supplementary figure 3B,C). Liver acyl-carnitine concentrations were similar between WT and KO mice (Figure 3B, and Supplementary Table ST1). Previously, somewhat higher concentrations of medium-chain liver acyl-carnitines have been reported in fasted MCAD-KO mice, albeit the difference was less pronounced than in blood [34].

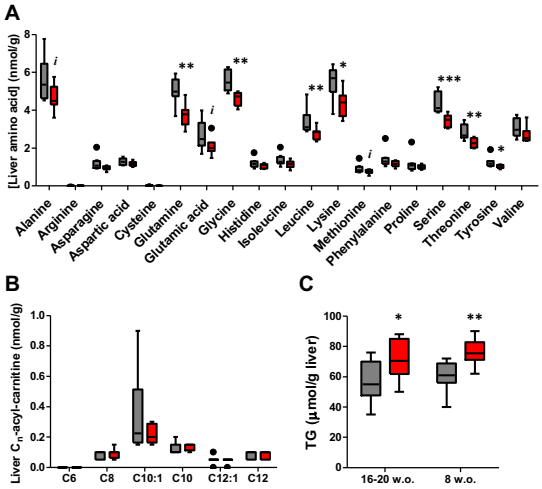

Figure 3. Hepatic metabolite profiles. Liver amino-acid (**A**) and C6-C12 acyl-carnitine concentrations for 8-weeks old mice (**B**), and liver triglyceride (TG) concentration of 16-20- and 8-weeks-old mice (**C**).

Apparently, cold-exposure triggers an adaptation of lipid metabolism in the MCAD-KO mice, leading to acyl-carnitine homeostasis. Finally, liver triglyceride (TG) concentrations were higher in the MCAD-KO than in the WT mice, in both age groups (Figure 3C), also suggesting altered lipid handling in the liver.

Rerouting of medium-chain acyl-CoAs into chain-elongation and triglyceride synthesis

The higher liver TG concentrations in the liver and comparable liver acyl-carnitine profiles suggest an altered lipid metabolism in the MCAD-KO mice. Therefore, we analyzed the lipids extracted from the liver by untargeted lipidomics. Over 600 single lipid species could be annotated, covering all major lipid classes (Figure 4A and Supplementary Table ST2). Principal Component Analysis (PCA) showed a clear separation between WT and MCAD-KO mice based on their hepatic lipid profiles (Figure 4B). The lipids that brought about the separation of the groups were almost exclusively TGs. The group of lipids with most pronounced differences between WT and KO ($p<0.05$ and fold change >2; Figure 4C upper right quadrant) consisted of 39 TGs, 1 diglyceride, and 1 sphingolipid (Supplementary table ST2). The TGs with the highest fold-changes, even up to 24-fold, had a sum of carbon atoms in the acyl chains in the range 40-48 (Figure 4D-H). This suggests that most of them contained at least one acyl chain shorter than C16. Subsequently, structural analysis revealed the acyl-chain composition of 31 out of the 42 lipids which were significantly elevated in MCAD-KO mice (upper right quadrant, Figure 4C. The *sn*-position of the acyl chains could not be determined. Over 130 TG isomers and 1 DG were annotated (Supplementary table ST3). 95% of the identified TG isomers contained at least one fatty-acyl chain with a carbon number in the range C6 to C14. 26% of these contained a second C14 fatty acyl-chain (Figure 4I). The majority of TGs contained at least one chain fatty acyl-residue ≥ C16. The deficiency of the MCAD enzyme mostly affects the oxidation of fatty acids of chain length C6-C10.

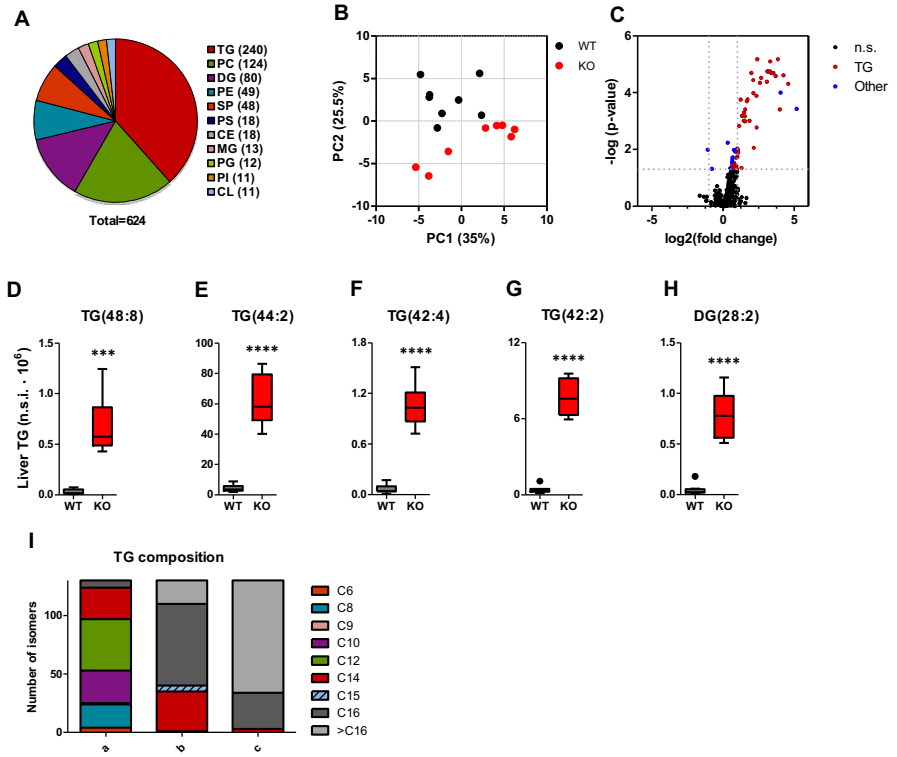

Figure 4. Hepatic lipidomics profile of 8-weeks old mice. Pie chart of identified lipid classes (**A**), PCA plot of identified lipid species for liver, with KO and WT mice depicted in red and black, respectively (**B**), Volcano plot of the identified lipid species for WT vs KO (**C**). Lipids for which the threshold of p<0.05 were not reached are depicted in black. For the other lipids, TGs are depicted in red and the remaining lipids in blue Tukey plots of the top 5 lipids (with the largest abundance difference between WT and KO (**D-H**), and the acyl-chain composition of differentially expressed TG isomers (**I**). Lipids in panel **I** were annotated as C(XX:Y), where C indicates lipid class, XX the total carbon numbers summed over all acyl chains, and Y the number of double bonds [36]. The acyl chains in each isomer were ordered from a to c, from shortest to longest chain length. ns: not significant, ***p<0.001, ****p<0.0001. n=8 per group. n.s.i. normalized signal intensity. See Figure 1 for further explanation of plots. See Supplementary Table ST2 for additional lipidomic results.

The lipidomics results suggest that some of the aberrant medium-chain fatty acyl-residues were incorporated into TGs, either directly or indirectly via partial chain elongation, thereby contributing to the prevention of their accumulation in the cells.

Zooming into an MCAD-KO mouse with a severe liver phenotype

Finally, we studied the KO mouse with the most extreme phenotype in more depth, considering that it may be a model for a human MCADD patient close to a metabolic crisis. We focused on severe hepatosteatosis (observed in MCADD patients who died of a metabolic crisis [37]) and on the effect of cold exposure on blood glucose. From qualitative and quantitative hepatohistological analyses and blood glucose change during cold exposure, we identified a KO mouse (KO10) with both severe steatohepatitis (*i.e.* inflammation of the liver

due to fat accumulation) (Figure 5A and Supplementary table ST4) and cold-induced decrease of the blood glucose concentration. This phenotype was specific for KO10, since neither a hepatopathological phenotype (Supplementary figure S4A) nor a reduction of the blood glucose concentration during cold exposure (Supplementary figure S4B) was typical of the MCAD-KO group. KO10 was the smallest KO mouse before cold exposure (18.4 g) and had the lowest body temperature at termination (21.3 °C). Two-dimensional clustering of selected sets of non-lipidomic metabolites (cf. materials and methods) showed that particularly the concentrations of hepatic amino acids and hepatic free and total carnitine were the lowest in KO10 compared to the other MCAD-KO mice (Figure 5B). All the amino acids in the corresponding cluster, except for leucine, are gluconeogenic. This suggests a shortage of substrate for gluconeogenesis and is in agreement with the lower blood glucose level in this KO mouse. In addition, the mouse has the lowest concentrations of methionine, histidine and L-cystathione, all of which contribute to the antioxidant capacity. Finally, this mouse had the lowest aspartate and serine levels of all MCAD-KO mice. These amino acids provide building blocks for purines, which are in turn building blocks for both CoASH and NAD^+. Both CoASH and NAD^+ are important cofactors for mFAO and are also involved in antioxidant and detoxification mechanisms.

Discussion

In this study, we investigated liver metabolism in mFAO deficient MCAD-KO mice during fasting and cold challenge, as a model for severe energetic stress. Until now, MCAD-KO mice were found to have a relatively mild phenotype and to maintain normal blood glucose levels during fasting. Previous RNASeq and proteomic analysis of liver tissue of fasted MCAD-KO liver tissue mice showed only minor adaptations [Martines et al. *Scientific Reports*, under revision], suggesting that the normal capacity of short- and long-chain isoenzymes (SCAD, LCAD, VLCAD) was sufficient to meet the hepatic energy demand during fasting. The more severe energetic stress imposed in this study – a combination of fasting and cold stress – revealed for the first time significantly lower blood glucose levels in MCAD-KO compared to WT mice. In contrast to an earlier study [10], we did not leave the mice in the cold until they died, since we were interested in their metabolic response before the energetic stress would be lethal. Apart from the lower blood glucose levels, compared to the WT mice, the MCAD-KO mice showed lower amino-acid levels in the liver but not in blood, higher blood NEFA levels, and higher storage of TGs containing C6-C14 acyl chains in the liver. In this section we will interpret our findings in the light of what is known about the role of the liver during cold stress. Then we will discuss how the observed differences in amino acid and lipid metabolism between the WT and KO mice obviate the metabolic consequences of MCAD deficiency. Finally, we will discuss the impact of our findings for patient pathophysiology.

Most studies on the role of mFAO during cold stress focus on BAT, the primary tissue responsible for non-shivering thermogenesis [14–16,20]. There is evidence, however, for a direct role of muscle [38] and liver [39] in non-shivering thermogenesis as well. The role of the liver to supply nutrients for BAT function has hardly been studied, but recently gained renewed interest [19,20]. Simcox et al. [19,20] revealed how cold exposure enhances lipolysis in white adipose tissue and supplies the liver with NEFAs.

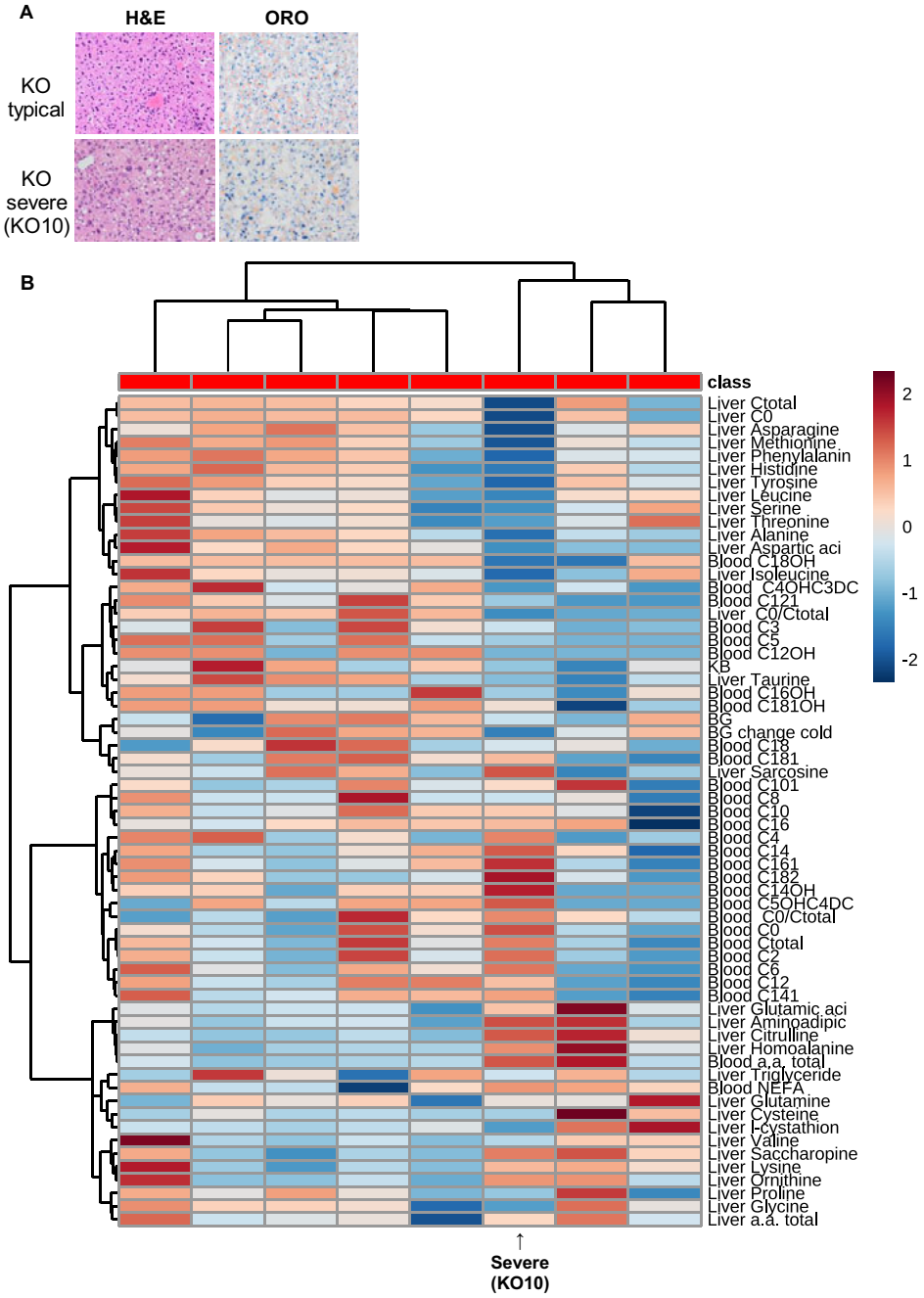

Figure 5. KO individual with extreme phenotype. Histological representation of a representative KO mouse liver and of the liver of the KO mouse with the most extreme phenotype (KO10) (**A**) and heat map of a selected set of metabolites in 8-weeks old MCAD-KO mice (**B**). Livers were stained by Haemotoxylin and Eosin (left) and Oil Red O (right).

In turn, the NEFAs activate liver mFAO and enhance secretion of acyl-carnitines into the bloodstream. These acyl-carnitines proved to be critical substrates for thermogenesis by BAT [19,20]. In our mice, *Mcad* deficiency led to higher levels of acyl-carnitines in the blood. It is likely that they serve as substrates for BAT, even though they may be only partly oxidized due to the *Mcad* deficiency. While we have no information about medium-chain mFAO capacity in BAT of the *Mcad*-deficient mice, it has been reported that mFAO genes, including *Acadvl, Acadl and Acadm* genes, are upregulated in BAT and livers of VLCAD- and LCAD-KO mice that have been fasted and cold-exposed [22].

The time courses of the body temperatures – with some mice showing minimal and some substantial temperature drops in both groups (Supplementary figures S1A-B) – suggest that we are able to bring only a subset of MCAD-KO mice to the brink of a metabolic collapse. This would explain why we observe a vast heterogeneity of body temperatures at the end of the cold period (Figures 1A and G). In this condition, we observed marked differences in amino-acid and lipid metabolism between the WT and KO mice. A limitation of this study is that we did not measure metabolic fluxes by isotope labelling. However, the comprehensive analysis of blood and liver metabolites already yields interesting insights in metabolic adaptations, as discussed below.

When the oxidation of fatty acids is deficient, amino acids may serve as an alternative substrate for oxidation and ATP production. Specific ketogenic amino acids (notably leucine and lysine) can also serve to replace fatty acids as a substrate for ketone-body production during fasting. Consistent with such increased utilization, most amino acid concentrations, including leucine and lysine, were substantially lower in MCAD-KO livers compared to WT mice, particularly in young mice (Figure 3A and Supplementary figure S3B). Blood ketone-body levels were not altered in MCAD-KO mice, suggesting that amino acids efficiently replaced fatty acids as substrates for ketogenesis. The fact that plasma amino acids were normal in the MCAD-KO mice, suggests that the hepatic amino-acid deficit originates in the liver and may be caused by an increased demand.

The higher plasma NEFA concentrations in MCAD-KO compared to WT mice is compatible with cold-induced lipolysis [19,20] in combination with a reduced fatty-acid utilization due to the MCAD deficiency. MCAD deficiency confers a risk of accumulation of medium-chain acyl-CoA esters and depletion of CoA. It has been hypothesized that this may cause the metabolic collapse of MCADD patients [40–42]. Interestingly, all lipidomic alterations that we observe in MCAD-KO mice, may be interpreted as a protection against such CoA depletion. First, we observed that liver acyl-carnitines were normal in MCAD-KO mice. Acyl-carnitines are often viewed as a reflection of their cognate acyl-CoA esters. This would suggest that MCAD-KO mice maintain acyl-CoA homeostasis under cold stress. Second, we observed increased acylcarnitine levels in the blood of MCAD-KO mice (Figure 2B-D). This is compatible with enhanced cold-induced acylcarnitine secretion from the liver [19,20] and would contribute to alleviating hepatic acyl-carnitine and acyl-CoA accumulation. In contrast, MCAD-KO mice that were only fasted, but not exposed to cold, did not maintain hepatic acyl-carnitine homeostasis [43], suggesting that acyl-carnitine secretion during cold-exposure adds to the homeostasis. Next, we observed higher TG levels, which was most pronounced for TGs containing C6-C14 acyl chains (Figure 4C-H). Incorporation of excess acyl moieties in TGs would also add to the prevention of acyl-CoA accumulation and subsequent CoA depletion. C6-C10 acyl-CoA esters are the preferred substrates of the MCAD enzyme and are

apparently also rerouted into TG synthesis. The increased C12-C14 acyl content of the TG pool can be explained either by direct rerouting of these intermediates from mFAO oxidation or by partial chain elongation of C6-C10 intermediates prior to their incorporation into TGs.

Finally, we wondered what is the relevance of this study for the understanding of human MCADD. The fact that only young MCAD-KO mice exhibited lower blood glucose levels than their wild-type counterparts during severe energetic stress, suggests that they are a good model for human disease. Also in human MCADD, untreated children are typically at risk of hypoglycemia during the first years of life when fasted in combination with an additional trigger, but less vulnerable when they grow older [44]. In human MCADD hypoketotic hypoglycemia is most often reported to occur upon a combination of fasting and intercurrent illness [1,6–9]. This is, however, difficult to mimic in the lab. There are also reports of cold sensitivity of MCADD patients [8,30,45], making cold stress a relevant and experimentally accessible laboratory intervention. Hypothesizing that the mouse with the most severe phenotype could yield insights into the processes during or close to a metabolic crisis, we zoomed in on MCAD-KO mouse 10 (KO10). This mouse showed both hepatosteatosis and a decrease of blood glucose concentration during cold exposure. This is in line with hepatosteatosis observed in MCADD patients who died from metabolic crisis (biochemically characterized by hypoketotic hypoglycemia). KO10 showed lower levels of the amino acids that contribute to the antioxidant capacity. Accordingly, lower antioxidant capacity has been reported in MCADD patients [46]. Therefore, when the blood glucose concentration in cold-exposed MCAD-KO mice drops, as observed in KO10, such mice may be adequate animal models for the onset of the metabolic crisis in human disease. Finally, KO10 had the lowest body temperature at termination. Since temperature can be followed continuously by the implanted loggers, it seems feasible to use it as a readout to study mice in a controlled way during more severe metabolic crisis.

We conclude that young, fasted, and cold exposed MCAD-KO mice are a relevant model for the onset of metabolic crisis in MCADD patients. We observed marked metabolic alterations in liver metabolism of cold-exposed fasted MCAD-KO mice. The results corroborate recent findings of the importance of hepatic fatty-acid metabolism during cold stress [19,20]. Alterations in amino acid and lipid metabolism are in line with a compensatory response in which amino acids partly take over the role of fatty acids as substrates for ATP and/or ketone body synthesis, and TG synthesis serves as a sink for excess acyl moieties, thereby preventing dangerous acyl-CoA accumulation [40–42].

Materials and Methods

Animals, Experimental design and Tissue sampling

Male MCAD-KO and wild-type (WT) mice on a C57BL/6J background (backcrossed for 10 generations [47]) were housed in a temperature- (21°C) and light-controlled facility. Mice were 16-20 weeks of age (young adult mice) or 8 weeks of age (young mice) at the start of the experiment. All experiments were approved by the Ethics Committee for Animal Experiments of the University of Groningen. Prior to the start of the experiment, mice were fed a chow-like semi-synthetic diet (D12450B, Research Diet Services, Wijk Bij Duurstede, The Netherlands) for 4-6 weeks, and had free access to drinking water. Subsequently, the mice were fasted for 14 hrs overnight and thereafter placed in a 5 °C environment for 4-6 hrs. The mice were terminated by cardiac puncture under isoflurane anesthesia. Two weeks before fasting, miniaturized Anipill Temperature Implant loggers (Data Sciences International,

Minnesota, USA) were implanted intraperitoneally under isoflurane and analgesia with flunixin/meglumine (2 mg/kg). At the end of the cold exposure and before termination, the body temperature was also measured with a rectal probe (Physitemp Instruments, Clifton, NJ, USA). During the experiment, blood glucose and ketone body concentrations were measured by a OneTouch UltraEasy® monitor (LifeScan Benelux, Beerse, Belgium) and Optium Xceed monitor (Abott Diabetes care Ltd UK), respectively. After termination the liver was removed quickly, weighed, and a piece of the liver freeze-clamped; a second piece was immersed in 10% buffered formalin and a third piece was fixated in Tissue-Tek® and frozen. Blood spots were taken immediately before fasting, at 14 hours after the start of fasting (i.e. before exposing the mice to cold) and at termination (after cold exposure).

Metabolite analysis

To determine hepatic triglyceride levels, freeze-clamped liver was crushed in liquid nitrogen. Subsequently 20% (w/v) liver homogenates were prepared in PBS (pH 7.4). Total liver lipids were extracted according to [48], redissolved in 2% Triton-X100 and analysed with a commercially available kit for triglyceride (Roche Diagnostics, Mannheim, Germany) according to the manufacturer's instructions. Amino-acid levels were measured according to Moore *et al.* [49]. Acyl-carnitine levels were measured according to Derks *et al.* [50]. NEFA concentratios were determined with a commercially available Diasys NEFA kit (Diasys Diagnostic Systems GmbH, Germany).

Liver lipid extraction

Liver tissue was homogenized in 0.9% NaCl to prepare a 20% (w/v) homogenate. We used a group of lipids (purchased from Avanti Polar lipids, Alabaster, AL) as internal standards for correcting the variation in lipid extraction and analytical analysis. Internal standards contain 4 nmol of each of the following lipids LPC (14:0), LPE (14:0),LPS(17:1), PC (17:0/17:0), PC(23:0/23:0), PE (14:0/14:0), PE(17:0/17:0), PS (17:0/17:0), PG (17:0/17:0), CL $(14:0)_4$, TG (19:2/19:2/19:2), CE (17:0), BMP (14:0) and 8nmol of LPG(14:0). Internal standards were dissolved in 200 µL $CHCl_3$:MeOH (1:1,v/v) and were added to each Eppendorf tube and pre-dried in vacuum centrifuge at 45°C before lipid extraction. Liver homogenate (50 µL corresponding to ≈10mg) was added to the tubes containing the pre-dried lipid standards. Lipid extraction was performed according to [51] with slight modification. In brief, 300 µL MeOH was mixed with 50 µL liver homogenate and bath-sonicated for 5 min. Subsequently, 1000 µL MTBE was added to the mixture and incubated on a shaker at 900 rpm for 20min at room temperature. Samples were centrifuged at 3000g for 10min to induce complete phase separation. The upper phase (900 µL) was transferred to a new tube. The lower phase was re-extracted with 600 µL MTBE/MeOH/H_2O(10:3:2.5, v/v/v). The combined 1400 µL upper phase was dried in a vacuum centrifuge at 45°C. The lipid pellet was dissolved in $CHCl_3$/MeOH(1:1,v/v) immediately prior to LC-MS measurement.

LC-MS measurement

Lipidomic analysis was performed on Ultimate 3000 high performance liquid chromatography (HPLC) coupled with Q-Exactive Orbitrap High Resolution Mass spectrometry (MS) (Thermo Scientific, Waltham, MA). LC separation was performed as described previously [52]. MS detection was done in positive electrospray ionization mode with data dependent MS/MS acquisition across the precursor ion range m/z 50−1750. One MS scan was performed followed directly by 10 MS/MS scans resulting in a duty cycle of ~1.2s. Resolution for full scan and fragment spectra acquisition were set at 70,000 and 17,500 FWHM, respectively. The source parameters were set as follows: source temperature 150 °C, spray voltage: 3.5kV, capillary temperature: 300 °C.

Lipidomic data analysis

Thermo Xcalibur® software (version 3.2.63 (Thermo Scientific, Waltham, MA) was used for data acquisition. Progenesis QI® software (Waters Corporation, Milford, MA) was used for data preprocessing including retention time alignment, peak picking and annotation of the LC-MS data. Peak picking was performed with an absolute ion intensity filter of 200,000 counts. Lipid annotation was performed by searching published lipid databases (Human Metabolome Database, Lipidmaps, Lipidblast) based on mass accuracy (<5ppm), isotopic similarities, adduct type, MS/MS spectra and elution behavior in comparison with known lipids of a home-made database. Analysis of the fatty-acyl composition of TG was performed using Lipidhunter2 software [53] with a predefined table of possible fragments (Supplementary table ST5). Lipid intensity was normalized to the intensity of the corresponding lipid standards in the same class. In case of the absence of lipid standards, the intensity was normalized to the average of all standards. Principle component analysis (PCA) was performed using MetaboAnalyst [54].

Histology

Formalin-fixed livers were processed for paraffin sectioning, and stained with hematoxylin and eosin. Frozen, Tissue-Tek® fixed livers were processed using standard methods and sections were stained with Oil-Red-O. The slides where scored for nonalcoholic fatty liver disease (NASH) according to Kleiner et al. [55].

Statistical analysis

The significance of differences, except for lipidomic data, were assessed using parametric (Student's t-test) or nonparametric tests (Mann Whitney U test) depending on their distribution. For changes in time, repeated-measures ANOVA was used. Untargeted lipidomic data were first log-transformed and subsequently differences were assessed with Student's t-test and adjusted for multiple comparison. A p value of <0.05 was considered statistically significant. Statistical analyses were performed using SPSS (v22) and the data was visualized using GraphPad Prism software (GraphPad Software Inc., version 5.00, 2007) and the MetaboAnalyst webserver [54].

Author contributions

AMFM, WZ, DJR, MG, RH and BMB designed the experiments. AMFM, AG and MG performed the animal experiments. AMFM, WZ, AG, JW, MK, LB, AB, MV, GV prepared and analyzed the samples. AMFM, WZ and MV analyzed the data. AMFM, WZ, JW, LB, AB, MG, RH, TD, DJR, BMB were involved in interpretation of results. AMFM, WZ, DJR, and BMB wrote the manuscript. All authors edited the manuscript.

Acknowledgements

This work was supported by the University Medical Center Groningen. The funders had no role in study design, data collection and analysis, decision to publish, or preparation of the manuscript. The authors like to thank Vincent W. Bloks for careful and independent checking of the statistical analysis and Marieke Smit for assisting with terminations.

Declaration of Interests

The authors declare no competing interests.

References

1. Rinaldo P, Matern D, Bennett MJ. Fatty Acid oxidation Disorders. Annu Rev Physiol. 2002;64(1):477–502.

2. Houten SM, Violante S, Ventura F V., Wanders RJA. The Biochemistry and Physiology of Mitochondrial Fatty Acid β-Oxidation and Its Genetic Disorders. Annu Rev Physiol. 2016;78(1):23–44.
3. Knottnerus SJG, Bleeker JC, Wüst RCI, Ferdinandusse S, Ijlst L, Wijburg FA, Wanders RJA, Visser G, Houtkooper RH. Disorders of mitochondrial long-chain fatty acid oxidation and the carnitine shuttle. 2018;
4. Derks TGJ, Van Spronsen FJ, Rake JP, Van Der Hilst CS, Span MM, Smit GPA. Safe and unsafe duration of fasting for children with MCAD deficiency. Eur J Pediatr. 2007;166(1):5–11.
5. Walter JH. Tolerance to fast: Rational and practical evaluation in children with hypoketonaemia. J Inherit Metab Dis. 2009;32(2):214–7.
6. Bennett MJ. Pathophysiology of fatty acid oxidation disorders. J Inherit Metab Dis. 2010;33(5):533–7.
7. Vishwanath VA. Fatty acid beta-oxidation disorders: A brief review. Ann Neurosci. 2016;23(1):51–5.
8. Schatz U a., Ensenauer R. The clinical manifestation of MCAD deficiency: Challenges towards adulthood in the screened population. J Inherit Metab Dis. 2010;33(5):513–20.
9. Volker-touw CML. MCAD deficiency To be , or not to be at risk. 2014.
10. Tolwani RJ, Hamm DA, Tian L, Sharer JD, Vockley J, Rinaldo P, Matern D, Schoeb TR, Wood PA. Medium-chain acyl-CoA dehydrogenase deficiency in gene-targeted mice. PLoS Genet. 2005;1(2):0205–12.
11. van Eunen K, Volker-Touw CML, Gerding A, Bleeker A, Wolters JC, van Rijt WJ, Martines A-CMF, Niezen-Koning KE, Heiner RM, Permentier H, Groen AK, Reijngoud D-J, Derks TGJ, Bakker BM. Living on the edge: substrate competition explains loss of robustness in mitochondrial fatty-acid oxidation disorders. BMC Biol. 2016;14(1):107.
12. Herrema H, Derks TGJ, Van Dijk TH, Bloks VW, Gerding A, Havinga R, Tietge UJF, M??ller M, Smit GPA, Kuipers F, Reijngoud DJ. Disturbed hepatic carbohydrate management during high metabolic demand in medium-chain acyl-CoA dehydrogenase (MCAD)-deficient mice. Hepatology. 2008;47(6):1894–904.
13. Spiekerkoetter U, Wood PA. Mitochondrial fatty acid oxidation disorders: Pathophysiological studies in mouse models. J Inherit Metab Dis. 2010;33(5):539–46.
14. Shibata H, Pérusse F, Vallerand a, Bukowiecki LJ. Cold exposure reverses inhibitory effects of fasting on peripheral glucose uptake in rats. Am J Physiol. 1989;257(1 Pt 2):R96–101.
15. López-Soriano FJ, Fernández-López JA, Mampel T, Villarroya F, Iglesias R, Alemany M. Amino acid and glucose uptake by rat brown adipose tissue. Effect of cold-exposure and acclimation. Biochem J. 1988;252(3):843–9.
16. Weir G, Ramage LE, Akyol M, Rhodes JK, Kyle CJ, Fletcher AM, Craven TH, Wakelin SJ, Drake AJ, Gregoriades ML, Ashton C, Weir N, van Beek EJR, Karpe F, Walker BR, Stimson RH. Substantial Metabolic Activity of Human Brown Adipose Tissue during Warm Conditions and Cold-Induced Lipolysis of Local Triglycerides. Cell Metab. 2018;27(6):1348-1355.e4.
17. Bartelt A, Bruns OT, Reimer R, Hohenberg H, Ittrich H, Peldschus K, Kaul MG, Tromsdorf UI, Weller H, Waurisch C, Eychmüller A, Gordts PLSM, Rinninger F, Bruegelmann K, Freund B, Nielsen P, Merkel M, Heeren J. Brown adipose tissue activity controls triglyceride clearance. Nat Med. 2011;17(2):200–6.
18. Shiota M, Tanaka T, Sugano T. Effect of norepinephrine on gluconeogenesis in perfused livers of cold-exposed rats. Am J Physiol Metab. 2017;249(3):E281–6.
19. Simcox J, Geoghegan G, Maschek JA, Bensard CL, Pasquali M, Miao R, Lee S, Jiang L, Huck I, Kershaw EE, Donato AJ, Apte U, Longo N, Rutter J, Schreiber R, Zechner R, Cox J, Villanueva CJ. Global Analysis of Plasma Lipids Identifies Liver-Derived Acylcarnitines as a Fuel Source for Brown Fat Thermogenesis. Cell Metab. 2017;26(3):509-522.e6.

20. Abumrad NA. The Liver as a Hub in Thermogenesis. Cell Metab. 2017;26(3):454–5.
21. Grefhorst A, van den Beukel JC, Dijk W, Steenbergen J, Voortman GJ, Leeuwenburgh S, Visser TJ, Kersten S, Friesema ECH, Themmen APN, Visser JA. Multiple effects of cold exposure on livers of male mice. J Endocrinol. 2018 Aug;238(2):91–106.
22. Goetzman ES, Tian L, Wood PA. Differential induction of genes in liver and brown adipose tissue regulated by peroxisome proliferator-activated receptor-α during fasting and cold exposure in acyl-CoA dehydrogenase-deficient mice. Mol Genet Metab. 2005;84(1):39–47.
23. Shore AM, Karamitri A, Kemp P, Speakman JR, Graham NS, Lomax MA. Cold-Induced Changes in Gene Expression in Brown Adipose Tissue, White Adipose Tissue and Liver. Lenburg M, editor. PLoS One. 2013 Jul 22;8(7):e68933.
24. Xiong D, He H, James J, Tokunaga C, Powers C, Huang Y, Osinska H, Towbin JA, Purevjav E, Balschi JA, Javadov S, McGowan FX, Strauss AW, Khuchua Z. Cardiac-specific VLCAD deficiency induces dilated cardiomyopathy and cold intolerance. AJP Hear Circ Physiol. 2014;306(3):H326–38.
25. Spiekerkoetter U, Tokunaga C, Wendel U, Mayatepek E, Exil V, Duran M, Wijburg FA, Wanders RJA, Strauss AW. Changes in blood carnitine and acylcarnitine profiles of very long-chain acyl-CoA dehydrogenase-deficient mice subjected to stress. Eur J Clin Invest. 2004;34(3):191–6.
26. Exil VJ. Abnormal mitochondrial bioenergetics and heart rate dysfunction in mice lacking very-long-chain acyl-CoA dehydrogenase. AJP Hear Circ Physiol. 2005;290(3):H1289–97.
27. Wolters JC, Ciapaite J, Van Eunen K, Niezen-Koning KE, Matton A, Porte RJ, Horvatovich P, Bakker BM, Bischoff R, Permentier HP. Translational Targeted Proteomics Profiling of Mitochondrial Energy Metabolic Pathways in Mouse and Human Samples. J Proteome Res. 2016;15(9):3204–13.
28. Herrema H, Derks TGJ, Van Dijk TH, Bloks VW, Gerding A, Havinga R, Tietge UJF, Müller M, Smit GPA, Kuipers F, Reijngoud DJ. Disturbed hepatic carbohydrate management during high metabolic demand in medium-chain acyl-CoA dehydrogenase (MCAD)-deficient mice. Hepatology. 2008;47(6):1894–904.
29. Vianey-Liaud C, Divry P, Gregersen N, Mathieu M. The inborn errors of mitochondrial fatty acid oxidation. J Inher Metab Dis. 1987;10:159–200.
30. Bentler K, Zhai S, Elsbecker SA, Arnold GL, Burton BK, Vockley J, Cameron CA, Hiner SJ, Edick MJ, Berry SA. 221 newborn-screened neonates with medium-chain acyl-coenzyme A dehydrogenase deficiency: Findings from the Inborn Errors of Metabolism Collaborative. Mol Genet Metab. 2016;119(1–2):75–82.
31. Walter JH. L-Carnitine in inborn errors of metabolism: What is the evidence? J Inherit Metab Dis. 2003;26(2–3):181–8.
32. Roe CR. Inherited disorders of mitochondrial fatty acid oxidation: A new responsibility for the neonatologist. Semin Neonatol. 2002;7(1):37–47.
33. Derks TGJ. MCAD deficiency : clinical and laboratory studies LK - https://rug.on.worldcat.org/oclc/150421504. [[S.l.] TA - TT -]: [s.n.]; 2007.
34. van Eunen K, Volker-Touw CML, Gerding A, Bleeker A, Wolters JC, van Rijt WJ, Martines A-CMF, Niezen-Koning KE, Heiner RM, Permentier H, Groen AK, Reijngoud D-J, Derks TGJ, Bakker BM. Living on the edge: substrate competition explains loss of robustness in mitochondrial fatty-acid oxidation disorders. BMC Biol. 2016;14(1):107.
35. Carpentier AC, Blondin DP, Virtanen KA, Richard D, Haman F, Turcotte ÉE. Brown adipose tissue energy metabolism in humans. Front Endocrinol (Lausanne). 2018;9(AUG):1–21.
36. Fahy E, Subramaniam S, Murphy RC, Nishijima M, Raetz CRH, Shimizu T, Spener F, van Meer G, Wakelam MJO, Dennis EA. Update of the LIPID MAPS comprehensive classification system for lipids. J Lipid Res. 2009;50(Supplement):S9–14.
37. Schatz UA, Ensenauer R. The clinical manifestation of MCAD deficiency: Challenges towards

adulthood in the screened population. J Inherit Metab Dis. 2010;33(5):513–20.
38. van Marken Lichtenbelt WD, Schrauwen P. Implications of nonshivering thermogenesis for energy balance regulation in humans. Am J Physiol Integr Comp Physiol. 2011;301(2):R285–96.
39. Stoner HB. The role of the liver in non-shivering thermogenesis in the rat. J Physiol. 1973 Jul;232(2):285–96.
40. Martines ACMF, van Eunen K, Reijngoud DJ, Bakker BM. The promiscuous enzyme medium-chain 3-keto-acyl-CoA thiolase triggers a vicious cycle in fatty-acid beta-oxidation. PLoS Comput Biol. 2017;13(4):1–22.
41. Mitchell GA, Gauthier N, Lesimple A, Wang SP, Mamer O, Qureshi I. Hereditary and acquired diseases of acyl-coenzyme A metabolism. Mol Genet Metab. 2008;94(1):4–15.
42. Yang H, Zhao C, Wang Y, Wang SP, Mitchell GA. Hereditary diseases of coenzyme A thioester metabolism. Biochem Soc Trans. 2019 Feb 28;47(1):149–55.
43. van Eunen K, Volker-Touw CML, Gerding A, Bleeker A, Wolters JC, van Rijt WJ, Martines A-CMF, Niezen-Koning KE, Heiner RM, Permentier H, Groen AK, Reijngoud D-J, Derks TGJ, Bakker BM. Living on the edge: substrate competition explains loss of robustness in mitochondrial fatty-acid oxidation disorders. BMC Biol. 2016;14(1):107.
44. Derks TGJ. MCAD deficiency: clinical and laboratory studies. s.n.; 2007. 163 p.
45. Ruitenbeek W, Poels PJE, Tumbull DM, Garavaglia B, Chalmers RA, Taylor RW. onset medium chain acyl-CoA dehydrogenase deficiency. 1995;209–14.
46. Derks TGJ, Touw CML, Ribas GS, Biancini GB, Vanzin CS, Negretto G, Mescka CP, Reijngoud DJ, Smit GPA, Wajner M, Vargas CR. Experimental evidence for protein oxidative damage and altered antioxidant defense in patients with medium-chain acyl-CoA dehydrogenase deficiency. J Inherit Metab Dis. 2014;37(5):783–9.
47. van Eunen K, Volker-Touw CML, Gerding A, Bleeker A, Wolters JC, van Rijt WJ, Martines ACMF, Niezen-Koning KE, Heiner RM, Permentier H, Groen AK, Reijngoud DJ, Derks TGJ, Bakker BM. Living on the edge: Substrate competition explains loss of robustness in mitochondrial fatty-acid oxidation disorders. BMC Biol. 2016;14(1):1–15.
48. Bligh EG, Dyer WJ. Canadian Journal of. Natl Res Counc Canada. 1959;37(8).
49. Moore S, Spackman DH, Stein WH. Chromatography of Amino Acids on Sulfonated Polystyrene Resins. An Improved System. Anal Chem. 1958 Jul;30(7):1185–90.
50. Derks TGJ, Boer TS, Assen A, Bos T, Ruiter J, Waterham HR, Niezen-Koning KE, Wanders RJA, Rondeel JMM, Loeber JG, Te Kate LP, Smit GPA, Reijngoud DJ. Neonatal screening for medium-chain acyl-CoA dehydrogenase (MCAD) deficiency in The Netherlands: The importance of enzyme analysis to ascertain true MCAD deficiency. J Inherit Metab Dis. 2008;31(1):88–96.
51. Matyash V, Liebisch G, Kurzchalia T V., Shevchenko A, Schwudke D. Lipid extraction by methyl-*tert* -butyl ether for high-throughput lipidomics. J Lipid Res. 2008;49(5):1137–46.
52. Gil A, Zhang W, Wolters JC, Permentier H, Boer T, Horvatovich P, Heiner-Fokkema MR, Reijngoud DJ, Bischoff R. One- vs two-phase extraction: re-evaluation of sample preparation procedures for untargeted lipidomics in plasma samples. Anal Bioanal Chem. 2018;410(23):5859–70.
53. Ni Z, Angelidou G, Lange M, Fedorova M. LipidHunter Identi fi es Phospholipids by High-Throughput Processing of LC-MS and Shotgun Lipidomics Datasets. 2017;
54. Chong J, Soufan O, Li C, Caraus I, Li S, Bourque G, Wishart DS, Xia J. MetaboAnalyst 4.0 : towards more transparent and integrative metabolomics analysis. Nucleic Acids Res. 2018;46(May):1–9.
55. Kleiner DE, Brunt EM, Van Natta M, Behling C, Contos MJ, Cummings OW, Ferrell LD, Liu YC, Torbenson MS, Unalp-Arida A, Yeh M, McCullough AJ, Sanyal AJ. Design and validation of a histological scoring system for nonalcoholic fatty liver disease. Hepatology. 2005;41(6):1313–

21.

Supplementary figures and tables

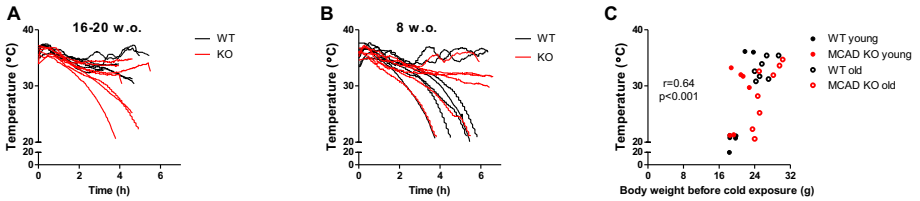

Suppl. Fig. S1. Rectal and body temperatures. Body temperature measured by intraperitoneally-implanted logger in the 16-20 (**A**) and 8 weeks old. mice (**B**), Body temperature versus body weight before cold exposure (**C**).

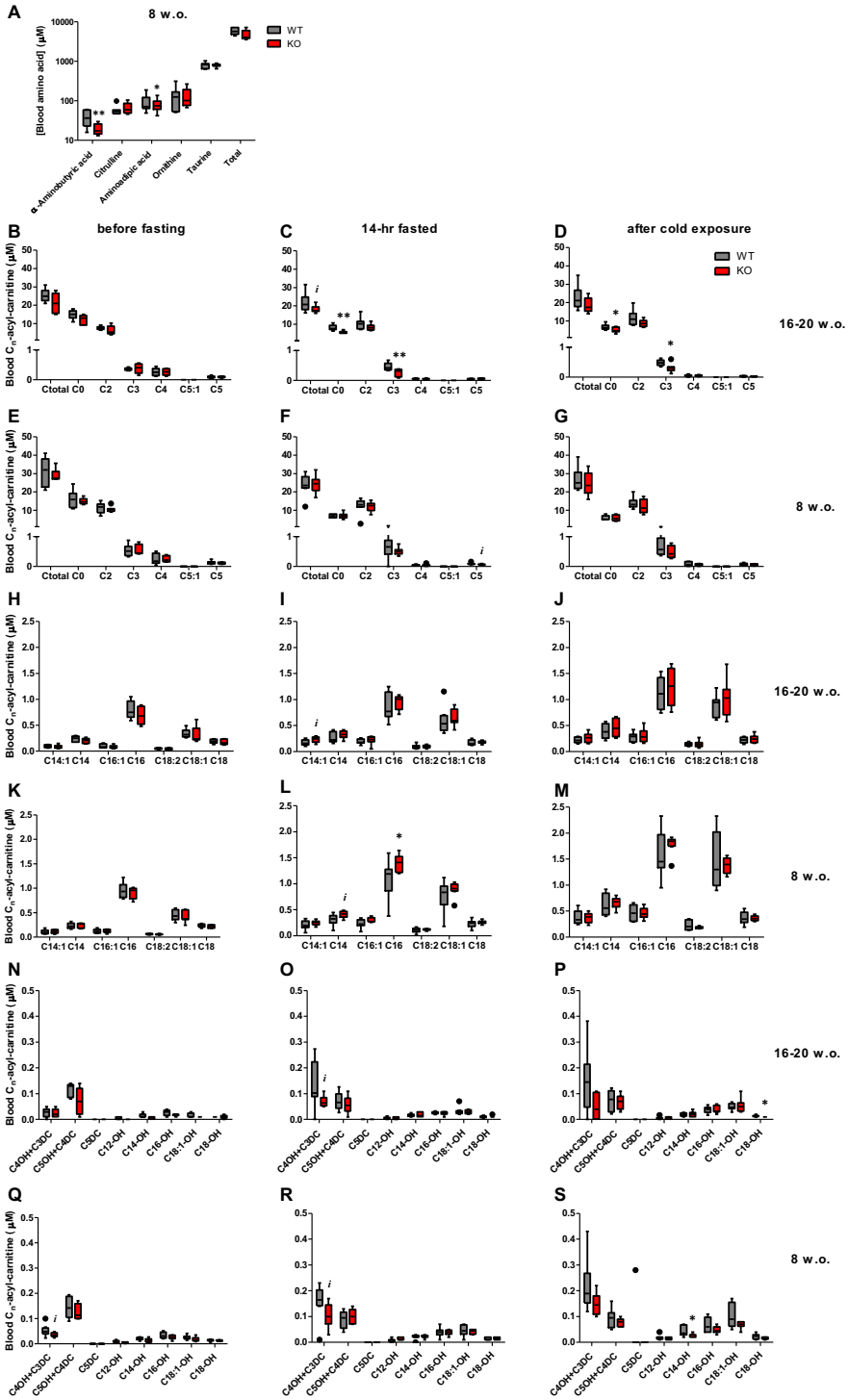

Suppl. Fig. S2. Blood non-proteomic amino acids and acyl-carnitine concentration.

Amino acid concentration 8 w.o, mice (**A**), Blood acyl-carnitine concentrations before fasting (**B,E,H,K,N,Q**), after 14 hrs of fasting, before cold exposure (**C,F,I,L,O,R**), and after fasting plus cold exposure (D,G,J,M,P,S) in 16-20-weeks-old (**B-D, H-J, N-P**) and 8-weeks-old mice (**B-D, H-J, N-P**).

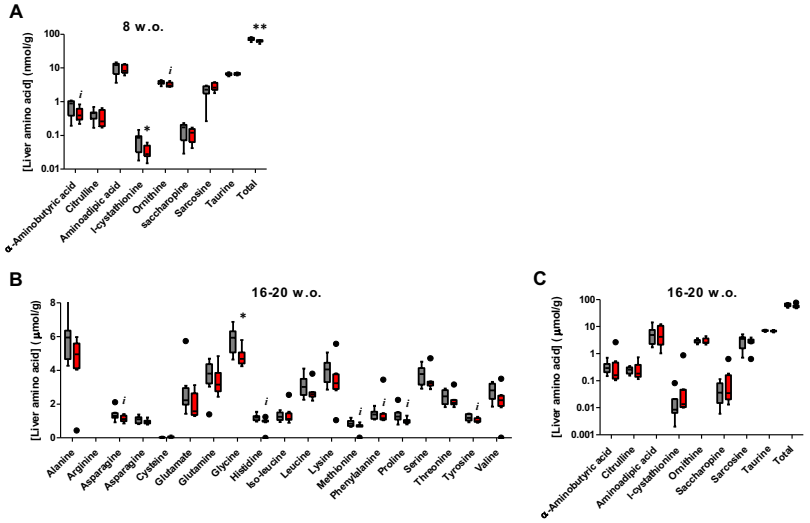

Suppl. Fig. S3. Non-proteomic liver amino acid levels of 8-weeks-old mice (A) and proteomic (B) and non-proteomic liver amino acid levels 16-20-weeks-old mice (C).

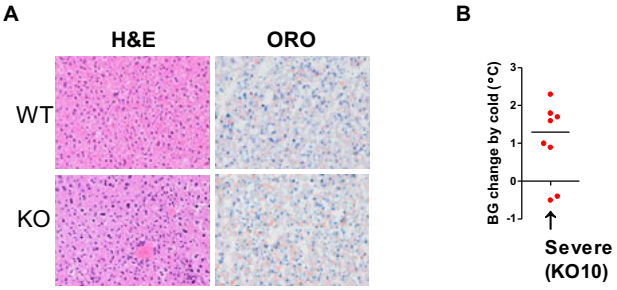

Suppl. Fig S4. Histological representation of representative WT and KO livers of 8-weeks-old mice (A) and blood glucose change during cold exposure in 8-weeks-old mice (B). Livers were stained by Haemotoxylin and Eosin (left) and Oil Red O (right).

Supplementary Table ST1. Biometric results and non-lipidomic metabolite concentrations of the WT and KO mice

	16-20 weeks-old				8 weeks-old				
	WT		KO		WT		KO		Tissue
Biometrics									
BW BF	29.10 ± 0.59		29.48 ± 0.95		22.51 ± 0.77		22.85 ± 0.51		
BW AF	26.19 ± 0.63		26.30 ± 0.94		19.59 ± 0.79		20.30 ± 0.54		
BW AFC	25.28 ± 0.61		25.79 ± 0.99		18.83 ± 0.68		19.50 ± 0.50		
BG BF	8.66 ± 0.27		7.88 ± 0.49		9.87 ± 0.39		9.06 ± 0.37		
BG AF	5.55 ± 0.30		4.84 ± 0.42		5.79 ± 0.58		4.58 ± 0.21	*i*	Blood
BG AFC	6.74 ± 0.60		6.53 ± 0.40		7.39 ± 0.52		5.63 ± 0.35	*	Blood
KB BF	0.31 ± 0.04		0.38 ± 0.03		0.45 ± 0.03		0.53 ± 0.07		Blood
KB AF	1.96 ± 0.27		1.48 ± 0.13		2.24 ± 0.19		1.88 ± 0.19		Blood
KB AFC	3.14 ± 0.36		2.70 ± 0.39		2.64 ± 0.14		2.35 ± 0.21		Blood
Logger_Temp BF	37.68 ± 0.31		36.86 ± 0.29		37.64 ± 0.25		36.93 ± 0.29		
Logger_Temp AF	36.27 ± 0.28		36.10 ± 0.25	*i*	35.43 ± 0.59		35.70 ± 0.29		
Logger_Temp AFC	33.30 ± 0.78		28.70 ± 2.21		25.09 ± 2.84		28.18 ± 2.24		

	16-20 weeks-old							8 weeks-old							
	WT			KO				WT			WT				Tissue
Rectal temperature	31.20	±	n.a.	28.20	±	n.a.		21.49	±	2.36	25.39	±	1.59		
Liver weight	1.06	±	0.04	1.23	±	0.05	*	0.89	±	0.04	1.04	±	0.03	*	
Relative liver weight	4.20	±	0.14	4.79	±	0.15	*	4.61	±	0.12	5.30	±	0.14	**	
Liver Triglycerides	56.75	±	4.76	71.25	±	4.65	*	60.63	±	3.58	76.38	±	3.05	**	Liver
Plasma NEFA	855	±	91	950	±	52		818	±	29	1036	±	62	**	Plasma
Blood acyl-carnitine concentrations before fasting															
Blood Ctotal BF	25.20	±	1.62	21.00	±	2.51		30.88	±	2.65	29.14	±	1.28		Blood
Blood C0 BF	15.00	±	1.14	12.00	±	1.26		15.88	±	1.62	15.00	±	0.62		Blood
Blood C2 BF	7.47	±	0.46	6.28	±	1.12		11.33	±	0.97	10.64	±	0.56		Blood
Blood C3 BF	0.35	±	0.02	0.38	±	0.07		0.53	±	0.07	0.57	±	0.07		Blood
Blood C4 BF	0.25	±	0.06	0.26	±	0.05		0.25	±	0.06	0.25	±	0.04		Blood
Blood C5:1 BF	0.00	±	0.00	0.00	±	0.00		0.00	±	0.00	0.00	±	0.00		Blood
Blood C5 BF	0.09	±	0.02	0.09	±	0.01		0.14	±	0.02	0.11	±	0.01		Blood
Blood C6 BF	0.03	±	0.00	0.07	±	0.02	*	0.03	±	0.01	0.10	±	0.02	*	Blood
Blood C8 BF	0.04	±	0.00	0.06	±	0.01	*	0.05	±	0.01	0.09	±	0.01	**	Blood
Blood C10:1 BF	0.02	±	0.00	0.05	±	0.02	**	0.02	±	0.00	0.08	±	0.01	**	Blood
Blood C10 BF	0.03	±	0.01	0.04	±	0.01		0.03	±	0.01	0.01	±	0.01		Blood
Blood C12:1 BF	0.02	±	0.00	0.03	±	0.00		0.02	±	0.00	0.02	±	0.00		Blood
Blood C12 BF	0.07	±	0.00	0.06	±	0.01		0.08	±	0.01	0.07	±	0.00		Blood
Blood C14:1 BF	0.09	±	0.01	0.08	±	0.02		0.11	±	0.01	0.11	±	0.01		Blood
Blood C14 BF	0.23	±	0.03	0.20	±	0.02		0.23	±	0.02	0.24	±	0.02		Blood
Blood C16:1 BF	0.10	±	0.02	0.08	±	0.02		0.12	±	0.02	0.12	±	0.01		Blood
Blood C16 BF	0.80	±	0.08	0.69	±	0.08		0.95	±	0.05	0.90	±	0.04		Blood
Blood C18:2 BF	0.05	±	0.01	0.04	±	0.01		0.06	±	0.00	0.06	±	0.00		Blood
Blood C18:1 BF	0.34	±	0.04	0.31	±	0.08		0.45	±	0.04	0.42	±	0.04		Blood
Blood C18 BF	0.19	±	0.02	0.18	±	0.02		0.24	±	0.01	0.22	±	0.01		Blood
Blood C4OH+C3DC BF	0.03	±	0.01	0.02	±	0.01		0.05	±	0.01	0.04	±	0.00	*i*	Blood
Blood C5OH+C4DC BF	0.11	±	0.01	0.07	±	0.02		0.14	±	0.01	0.13	±	0.01		Blood
Blood C5DC BF	0.00	±	0.00	0.00	±	0.00		0.00	±	0.00	0.00	±	0.00		Blood
Blood C12OH BF	0.00	±	0.00	0.00	±	0.00		0.01	±	0.00	0.01	±	0.00		Blood
Blood C14OH BF	0.01	±	0.00	0.01	±	0.00		0.02	±	0.00	0.02	±	0.00		Blood
Blood C16OH BF	0.03	±	0.01	0.02	±	0.00		0.03	±	0.00	0.02	±	0.00		Blood
Blood C18:1OH BF	0.02	±	0.00	0.01	±	0.00		0.03	±	0.00	0.02	±	0.00		Blood
Blood C18OH BF	0.01	±	0.00	0.01	±	0.00		0.01	±	0.00	0.01	±	0.00		Blood
Blood C0/Ctotal BF	0.59	±	0.02	0.58	±	0.02		0.52	±	0.02	0.50	±	0.01		Blood
Blood acyl-carnitine concentrations 14 hrs of fasting															
Blood Ctotal AF	21.86	±	1.79	18.13	±	0.69	*i*	23.75	±	2.02	24.25	±	1.62		Blood
Blood C0 AF	8.09	±	0.54	5.75	±	0.25	**	7.00	±	0.33	7.00	±	0.53		Blood
Blood C2 AF	10.31	±	1.14	8.31	±	0.61		12.23	±	1.50	12.03	±	0.90		Blood
Blood C3 AF	0.46	±	0.05	0.26	±	0.04	**	0.68	±	0.16	0.51	±	0.04		Blood
Blood C4 AF	0.05	±	0.00	0.05	±	0.01		0.05	±	0.01	0.04	±	0.01		Blood
Blood C5:1 AF	0.00	±	0.00	0.00	±	0.00		0.00	±	0.00	0.00	±	0.00		Blood
Blood C5 AF	0.05	±	0.00	0.05	±	0.01		0.09	±	0.01	0.07	±	0.01	*i*	Blood
Blood C6 AF	0.02	±	0.00	0.13	±	0.01	****	0.03	±	0.00	0.12	±	0.03	***	Blood
Blood C8 AF	0.04	±	0.01	0.11	±	0.01	***	0.06	±	0.00	0.15	±	0.01	****	Blood
Blood C10:1 AF	0.03	±	0.00	0.19	±	0.02	****	0.02	±	0.00	0.22	±	0.02	***	Blood
Blood C10 AF	0.04	±	0.00	0.07	±	0.00	***	0.03	±	0.01	0.08	±	0.01	**	Blood
Blood C12:1 AF	0.03	±	0.00	0.05	±	0.01	*	0.03	±	0.00	0.05	±	0.01	*	Blood
Blood C12 AF	0.06	±	0.01	0.09	±	0.01	*i*	0.08	±	0.01	0.11	±	0.01	*i*	Blood
Blood C14:1 AF	0.17	±	0.02	0.23	±	0.02	*i*	0.21	±	0.03	0.25	±	0.02		Blood
Blood C14 AF	0.27	±	0.04	0.33	±	0.03		0.31	±	0.04	0.41	±	0.02	*i*	Blood
Blood C16:1 AF	0.19	±	0.02	0.22	±	0.03		0.24	±	0.03	0.30	±	0.02		Blood
Blood C16 AF	0.87	±	0.09	0.95	±	0.05		1.09	±	0.13	1.40	±	0.06	*	Blood
Blood C18:2 AF	0.09	±	0.01	0.09	±	0.01		0.11	±	0.02	0.12	±	0.01		Blood
Blood C18:1 AF	0.60	±	0.09	0.65	±	0.06		0.76	±	0.10	0.89	±	0.05		Blood
Blood C18 AF	0.17	±	0.02	0.18	±	0.01		0.23	±	0.03	0.27	±	0.01		Blood
Blood C4OH+C3DC AF	0.13	±	0.03	0.07	±	0.01	*i*	0.16	±	0.02	0.10	±	0.02	*i*	Blood
Blood C5OH+C4DC AF	0.07	±	0.01	0.06	±	0.01		0.09	±	0.01	0.10	±	0.01		Blood
Blood C5DC AF	0.00	±	0.00	0.00	±	0.00		0.00	±	0.00	0.00	±	0.00		Blood
Blood C12OH AF	0.01	±	0.00	0.00	±	0.00		0.01	±	0.00	0.01	±	0.00		Blood

	16-20 weeks-old							8 weeks-old							
	WT			KO				WT			WT				Tissue
Blood C14OH AF	0.02	±	0.00	0.02	±	0.00		0.02	±	0.00	0.02	±	0.00		Blood
Blood C16OH AF	0.03	±	0.00	0.03	±	0.00		0.04	±	0.01	0.04	±	0.00		Blood
Blood C18:1OH AF	0.03	±	0.01	0.03	±	0.00		0.05	±	0.01	0.04	±	0.00		Blood
Blood C18OH AF	0.01	±	0.00	0.01	±	0.00		0.01	±	0.00	0.02	±	0.00		Blood
Blood C0/Ctotal AF	0.38	±	0.02	0.33	±	0.02		0.32	±	0.05	0.29	±	0.01		Blood
Blood acyl-carnitine concentrations after fasting and cold exposure															
Blood Ctotal AFC	22.70	±	2.20	18.63	±	1.40		26.63	±	2.17	24.50	±	2.16		Blood
Blood C0 AFC	6.67	±	0.53	5.00	±	0.53	*	5.88	±	0.44	5.75	±	0.56		Blood
Blood C2 AFC	11.65	±	1.48	8.76	±	0.67		13.90	±	1.03	12.13	±	1.31		Blood
Blood C3 AFC	0.48	±	0.04	0.31	±	0.05	*	0.64	±	0.10	0.47	±	0.07		Blood
Blood C4 AFC	0.05	±	0.01	0.05	±	0.01		0.08	±	0.02	0.05	±	0.01		Blood
Blood C5:1 AFC	0.00	±	0.00	0.00	±	0.00		0.00	±	0.00	0.00	±	0.00		Blood
Blood C5 AFC	0.03	±	0.01	0.02	±	0.00		0.07	±	0.01	0.05	±	0.01		Blood
Blood C6 AFC	0.02	±	0.00	0.08	±	0.01		0.02	±	0.01	0.08	±	0.02	**	Blood
Blood C8 AFC	0.04	±	0.01	0.09	±	0.01		0.05	±	0.01	0.14	±	0.01	***	Blood
Blood C10:1 AFC	0.02	±	0.00	0.18	±	0.02		0.02	±	0.00	0.23	±	0.02	***	Blood
Blood C10 AFC	0.04	±	0.00	0.07	±	0.01		0.04	±	0.01	0.08	±	0.01	*	Blood
Blood C12:1 AFC	0.03	±	0.00	0.04	±	0.00		0.04	±	0.00	0.05	±	0.01		Blood
Blood C12 AFC	0.07	±	0.01	0.09	±	0.01		0.11	±	0.01	0.12	±	0.01		Blood
Blood C14:1 AFC	0.22	±	0.02	0.26	±	0.03		0.38	±	0.05	0.37	±	0.03		Blood
Blood C14 AFC	0.39	±	0.05	0.46	±	0.06		0.61	±	0.07	0.66	±	0.04		Blood
Blood C16:1 AFC	0.27	±	0.03	0.31	±	0.05		0.46	±	0.05	0.46	±	0.04		Blood
Blood C16 AFC	1.12	±	0.11	1.26	±	0.13		1.60	±	0.16	1.78	±	0.06		Blood
Blood C18:2 AFC	0.14	±	0.01	0.14	±	0.02		0.23	±	0.03	0.18	±	0.01		Blood
Blood C18:1 AFC	0.87	±	0.08	1.02	±	0.13		1.47	±	0.19	1.38	±	0.05		Blood
Blood C18 AFC	0.22	±	0.02	0.24	±	0.03	*	0.37	±	0.04	0.36	±	0.02		Blood
Blood C4OH+C3DC AFC	0.15	±	0.04	0.05	±	0.02		0.22	±	0.04	0.15	±	0.01		Blood
Blood C5OH+C4DC AFC	0.07	±	0.01	0.07	±	0.01		0.09	±	0.01	0.08	±	0.01		Blood
Blood C5DC AFC	0.00	±	0.00	0.00	±	0.00		0.04	±	0.04	0.00	±	0.00		Blood
Blood C12OH AFC	0.01	±	0.00	0.01	±	0.00		0.02	±	0.00	0.02	±	0.00		Blood
Blood C14OH AFC	0.02	±	0.00	0.02	±	0.00		0.04	±	0.01	0.03	±	0.00		Blood
Blood C16OH AFC	0.04	±	0.00	0.04	±	0.01		0.07	±	0.01	0.05	±	0.00		Blood
Blood C18:1OH AFC	0.05	±	0.00	0.05	±	0.01		0.10	±	0.02	0.07	±	0.00		Blood
Blood C18OH AFC	0.01	±	0.00	0.01	±	0.00		0.02	±	0.00	0.02	±	0.00		Blood
Blood C0/Ctotal AFC	0.30	±	0.01	0.27	±	0.02		0.23	±	0.01	0.23	±	0.00		Blood
Liver acyl-carnitine concentrations (after fasting and cold exposure)															
Liver Ctotal	300	±	11	284	±	21		336	±	17	324	±	12		Liver
Liver C0	284	±	9	271	±	21		311	±	18	303	±	13		Liver
Liver C2	4.84	±	1.72	2.73	±	1.35		9.26	±	2.21	5.51	±	1.62		Liver
Liver C3	1.93	±	0.38	1.89	±	0.36		3.48	±	0.58	3.26	±	0.35		Liver
Liver C4	0.24	±	0.05	0.10	±	0.02		0.30	±	0.05	0.29	±	0.06		Liver
Liver C5:1	0.08	±	0.01	0.04	±	0.01		0.09	±	0.01	0.06	±	0.01		Liver
Liver C5	0.21	±	0.11	0.08	±	0.01		0.16	±	0.03	0.12	±	0.01		Liver
Liver C6	0.00	±	0.00	0.00	±	0.00		0.00	±	0.00	0.00	±	0.00		Liver
Liver C8	0.08	±	0.01	0.05	±	0.01	*i*	0.08	±	0.01	0.09	±	0.01		Liver
Liver C10:1	0.24	±	0.05	0.20	±	0.02		0.34	±	0.10	0.22	±	0.02		Liver
Liver C10	0.11	±	0.01	0.11	±	0.02		0.13	±	0.01	0.14	±	0.01		Liver
Liver C12:1	0.05	±	0.01	0.03	±	0.01		0.05	±	0.01	0.04	±	0.01		Liver
Liver C12	0.06	±	0.01	0.06	±	0.01		0.08	±	0.01	0.08	±	0.01		Liver
Liver C14:1	0.09	±	0.01	0.08	±	0.01		0.09	±	0.01	0.08	±	0.01		Liver
Liver C14	0.04	±	0.01	0.03	±	0.01		0.08	±	0.01	0.05	±	0.00		Liver
Liver C16:1	0.06	±	0.02	0.05	±	0.02		0.08	±	0.01	0.06	±	0.01		Liver
Liver C16	0.16	±	0.02	0.13	±	0.03		0.26	±	0.04	0.19	±	0.03		Liver
Liver C18:2	0.09	±	0.01	0.08	±	0.01		0.09	±	0.01	0.10	±	0.01		Liver
Liver C18:1	0.21	±	0.03	0.16	±	0.04		0.24	±	0.03	0.22	±	0.03		Liver
Liver C18	0.07	±	0.01	0.07	±	0.01		0.12	±	0.01	0.08	±	0.01	*	Liver
Liver C4OH+C3DC	3.17	±	0.32	1.86	±	0.13		3.98	±	0.25	2.25	±	0.08	***	Liver
Liver C5OH+C4DC	0.77	±	0.06	0.58	±	0.04		0.89	±	0.05	0.70	±	0.04	*	Liver
Liver C5DLiver C	2.92	±	0.33	4.76	±	0.96		4.96	±	0.34	7.70	±	0.76	**	Liver
Liver C12OH	0.00	±	0.00	0.00	±	0.00		0.00	±	0.00	0.00	±	0.00		Liver

	16-20 weeks-old						8 weeks-old						
	WT			KO			WT			WT			Tissue
Liver C14OH	0.00	±	0.00	0.00	±	0.00	0.00	±	0.00	0.00	±	0.00	Liver
Liver C16OH	0.04	±	0.01	0.00	±	0.00	0.06	±	0.01	0.04	±	0.01	Liver
Liver C18:1OH	0.00	±	0.00	0.00	±	0.00	0.00	±	0.00	0.00	±	0.00	Liver
Liver C18OH	0.00	±	0.00	0.00	±	0.00	0.00	±	0.00	0.00	±	0.00	Liver
Liver C0/Ctotal	0.95	±	0.01	0.95	±	0.01	0.92	±	0.01	0.93	±	0.01	Liver
Liver amino acid concentrations (after fasting and cold exposure)													
Alanine	5914	±	508	4466	±	620	5643	±	399	4706	±	252 *i*	Liver
Arginine	n.d.	±	n.d.	n.d.	±	n.d.	37	±	21	18	±	3	Liver
Asparagine	1367	±	122	1132	±	66	1200	±	131	947	±	42	Liver
Aspartic acid	1064	±	73	941	±	47	1289	±	61	1161	±	47	Liver
Cysteine	23.6	±	10.4	41.0	±	20.2	31.5	±	9.9	12.3	±	5.2	Liver
Glutamine	2652	±	474	1918	±	252	5012	±	248	3760	±	214 **	Liver
Glutamic acid	3625	±	366	3343	±	273	2675	±	267	2095	±	173 *i*	Liver
Glycine	5805	±	266	4799	±	177 **	5560	±	191	4605	±	124 **	Liver
Histidine	1200	±	66	900	±	133 *	1199	±	93	1066	±	44	Liver
Isoleucine	1275	±	88	1315	±	187	1368	±	112	1149	±	70	Liver
Leucine	3059	±	212	2691	±	169	3395	±	233	2780	±	113 **	Liver
Lysine	3944	±	255	3296	±	441	5490	±	297	4338	±	265 *	Liver
Methionine	866	±	64	645	±	95 *i*	914	±	84	751	±	41 *i*	Liver
Phenylalanine	1385	±	97	1470	±	286	1426	±	163	1181	±	57	Liver
Proline	1329	±	152	980	±	56 *	1183	±	169	1006	±	42	Liver
Serine	3720	±	198	3360	±	199	4364	±	194	3466	±	113 ***	Liver
Threonine	2415	±	148	2194	±	146	2840	±	141	2272	±	81 **	Liver
Tyrosine	1203	±	70	1030	±	47 *i*	1262	±	102	1034	±	32 *	Liver
Valine	2718	±	182	2100	±	345	3069	±	169	2746	±	155	Liver
Aminoadipic acid	5751	±	1448	5743	±	1573	10473	±	1390	9075	±	969	Liver
α-Aminobutyric acid	334	±	64	512	±	305	767	±	124	438	±	76 *i*	Liver
Citrulline	247	±	25	279	±	74	426	±	54	339	±	68	Liver
l-cystathionine	19	±	9	127	±	106	76	±	15	34	±	6 *	Liver
Ornithine	2939	±	169	2927	±	292	3759	±	177	3275	±	190 *i*	Liver
Saccharopine	47	±	13	129	±	75	152	±	27	108	±	18	Liver
Sarcosine	3065	±	535	2787	±	352	2120	±	316	2750	±	259	Liver
Taurine	7110	±	153	6863	±	164	6591	±	209	6656	±	158 *i*	Liver
Total amino acids	63075	±	2906	55987	±	3275	72297	±	2749	61757	±	1857 **	Liver
Plasma amino acid concentrations (after fasting and cold exposure)													
Alanine							333	±	72	283	±	50	Plasma
Arginine							86	±	15	75	±	8	Plasma
Asparagine							58	±	10	51	±	7	Plasma
Cystine							8	±	5	7	±	2	Plasma
Glutamate							25.5	±	6.3	23.4	±	2.3	Plasma
Glutamine							639	±	73	611	±	49	Plasma
Glycine							222	±	41	191	±	37	Plasma
Histidine							94	±	25	103	±	20	Plasma
Isoleucine							183	±	17	175	±	6	Plasma
Leucine							498	±	89	402	±	48	Plasma
Lysine							599	±	121	436	±	69	Plasma
Methionine							52	±	9	38	±	4	Plasma
Phenylalanine							135	±	33	138	±	24	Plasma
Proline							88	±	19	74	±	10	Plasma
Serine							147	±	30	127	±	23	Plasma
Threonine							267	±	40	200	±	18	Plasma
Tryptophan							41	±	8	42	±	4	Plasma
Tyrosine							188	±	65	130	±	34	Plasma
Valine							591	±	92	524	±	57	Plasma
Aminoadipic acid							94	±	18	81	±	10	Plasma
α-Aminobutyric acid							40	±	6	20	±	2 *	Plasma
Citrulline							59	±	7	66	±	8	Plasma
Ornithine							138	±	34	130	±	25	Plasma
Taurine							813	±	52	799	±	26	Plasma
Total amino acids							5397	±	835	4726	±	495	Plasma

BF: Before fasting, AF: After 14 hours of fasting, AFC: After fasting and cold exposure, BW: Body weights, BG: Blood glucose, KB: Ketone bodies, i: p<0.1 vs WT, *: p<0.05 vs WT, **: p<0.01 vs WT, ***: p<0.001 vs WT, ****: p<0.0001 vs WT. The values are expressed as average ± SEM. n = 5-8.

Supplementary Table ST2. Lipidomic profile results in livers of 8-week-old mice.

Lipid Class	ID	Name	Mean MCAD-KO	Mean WT	p-value	Adjusted p-value	Fold change	Threshold
TG	TG20	TG(46:6)	2.2E+06	4.1E+05	3.2E-08	6.7E-06	5.28	Up
SP	SP17	HexCer(d46:3)	1.1E+06	1.1E+05	2.5E-08	6.7E-06	10.77	Up
TG	TG43	TG(44:2)	6.2E+07	4.3E+06	2.2E-08	6.7E-06	14.46	Up
TG	TG25	TG(48:7)	9.2E+06	9.2E+05	5.1E-08	8.0E-06	10.01	Up
TG	TG13	TG(40:2)	3.2E+06	3.7E+05	1.7E-07	1.8E-05	8.65	Up
TG	TG16	TG(46:6)	2.7E+06	3.0E+05	1.9E-07	1.8E-05	9.16	Up
TG	TG15	TG(42:3)	8.6E+06	8.8E+05	2.0E-07	1.8E-05	9.88	Up
TG	TG27	TG(40:0)	4.0E+05	1.0E+05	2.7E-07	2.0E-05	3.97	Up
TG	TG28	TG(44:3)	7.6E+07	7.2E+06	3.2E-07	2.0E-05	10.49	Up
TG	TG19	TG(44:4)	1.9E+07	1.6E+06	3.0E-07	2.0E-05	11.69	Up
TG	TG24	TG(42:2)	7.7E+06	4.1E+05	4.4E-07	2.5E-05	18.95	Up
TG	TG14	TG(44:5)	3.1E+06	2.3E+05	5.1E-07	2.6E-05	13.03	Up
TG	TG23	TG(46:5)	1.3E+07	2.0E+06	6.4E-07	3.1E-05	6.37	Up
TG	TG45	TG(43:1)	3.7E+05	8.6E+04	8.2E-07	3.6E-05	4.35	Up
TG	TG18	TG(40:1)	4.2E+06	5.0E+05	1.0E-06	4.1E-05	8.50	Up
TG	TG22	TG(42:2)	1.6E+07	2.6E+06	1.2E-06	4.5E-05	6.05	Up
TG	TG17	TG(48:8)	6.9E+05	2.9E+04	1.3E-06	4.9E-05	24.06	Up
DG	DG3	DG(28:2)	7.8E+05	4.7E+04	2.9E-06	1.0E-04	16.53	Up
TG	TG30	TG(46:4)	5.1E+07	1.2E+07	3.2E-06	1.0E-04	4.39	Up
TG	TG32	TG(42:1)	2.0E+07	4.0E+06	4.2E-06	1.3E-04	5.11	Up
TG	TG31	TG(48:6)	6.9E+06	2.1E+06	5.8E-06	1.7E-04	3.31	Up
TG	TG55	TG(42:0)	1.3E+06	5.6E+05	6.2E-06	1.7E-04	2.37	Up
TG	TG35	TG(44:2)	4.5E+07	1.4E+07	7.4E-06	2.0E-04	3.18	Up
TG	TG26	TG(50:8)	2.9E+06	9.9E+05	1.5E-05	3.9E-04	2.96	Up
TG	TG12	TG(42:4)	1.1E+06	6.6E+04	1.6E-05	3.9E-04	15.95	Up
TG	TG44	TG(46:3)	1.9E+07	6.8E+06	2.1E-05	5.0E-04	2.80	Up
TG	TG33	TG(48:6)	3.4E+06	1.3E+06	2.9E-05	6.7E-04	2.52	Up
TG	TG53	TG(46:3)	3.8E+07	1.3E+07	3.1E-05	6.8E-04	2.90	Up
TG	TG61	TG(44:1)	4.6E+07	1.7E+07	4.7E-05	9.8E-04	2.75	Up
TG	TG21	TG(48:7)	3.0E+06	8.3E+05	4.7E-05	9.8E-04	3.65	Up
TG	TG52	TG(47:6)	2.6E+05	8.8E+04	5.2E-05	1.0E-03	2.94	Up
TG	TG54	TG(45:2)	2.4E+06	1.1E+06	7.7E-05	1.5E-03	2.20	Up
TG	TG34	TG(45:3)	5.0E+05	9.6E+04	8.9E-05	1.7E-03	5.16	Up
PL	PL67	PC(44:0)	3.2E+05	2.5E+05	3.2E-04	5.8E-03	1.26	Not
TG	TG36	TG(47:5)	2.9E+06	6.5E+05	4.9E-04	8.8E-03	4.48	Up
TG	TG66	TG(46:2)	2.0E+08	1.0E+08	5.4E-04	9.3E-03	2.01	Up
PL	PL78	PC(O-38:1)	8.3E+04	1.7E+05	6.1E-04	1.0E-02	0.48	Down
PL	PL7	PC(32:2)	7.4E+06	4.4E+06	6.7E-04	1.1E-02	1.70	Not
TG	TG37	TG(48:5)	3.3E+07	1.8E+07	6.8E-04	1.1E-02	1.86	Not
TG	TG40	TG(50:7)	4.4E+06	2.1E+06	6.7E-04	1.1E-02	2.07	Up
PL	PL2	PC(30:1)	6.9E+05	3.8E+05	7.9E-04	1.2E-02	1.81	Not
TG	TG51	TG(50:6)	1.6E+07	7.8E+06	8.6E-04	1.3E-02	2.09	Up
TG	TG73	TG(45:1)	2.1E+06	1.0E+06	9.0E-04	1.3E-02	2.06	Up
TG	TG59	TG(48:4)	7.0E+07	3.5E+07	1.3E-03	1.8E-02	2.01	Up
PL	PL8	PC(32:3)	2.2E+05	1.4E+05	1.4E-03	1.9E-02	1.60	Not
TG	TG88	TG(46:1)	1.9E+08	9.7E+07	1.5E-03	2.0E-02	1.91	Not
CL	CL9	CL(70:5)	2.0E+06	1.3E+06	1.7E-03	2.3E-02	1.58	Not
PL	PL18	PC(34:4)	2.7E+06	1.8E+06	2.2E-03	2.8E-02	1.55	Not
TG	TG84	TG(44:0)	5.7E+06	3.3E+06	2.4E-03	3.0E-02	1.74	Not
TG	TG39	TG(50:7)	8.4E+06	5.0E+06	2.5E-03	3.1E-02	1.67	Not
TG	TG74	TG(48:3)	1.6E+08	1.0E+08	2.9E-03	3.5E-02	1.55	Not
TG	TG82	TG(47:2)	1.1E+07	6.6E+06	3.4E-03	4.0E-02	1.73	Not
TG	TG97	TG(48:2)	1.1E+09	6.2E+08	3.3E-03	4.0E-02	1.74	Not
TG	TG65	TG(47:3)	3.2E+06	1.7E+06	3.4E-03	4.0E-02	1.92	Not
TG	TG62	TG(50:6)	8.1E+06	4.6E+06	3.8E-03	4.3E-02	1.75	Not
TG	TG77	TG(52:6)	3.3E+08	2.0E+08	4.0E-03	4.4E-02	1.63	Not
TG	TG60	TG(48:4)	6.9E+07	4.5E+07	4.2E-03	4.5E-02	1.53	Not
TG	TG64	TG(52:7)	5.0E+07	2.9E+07	4.3E-03	4.5E-02	1.71	Not
TG	TG42	TG(47:4)	6.2E+05	2.5E+05	4.3E-03	4.5E-02	2.46	Up
PL	PL19	PC(34:4)	1.9E+06	1.3E+06	4.4E-03	4.6E-02	1.43	Not
TG	TG115	TG(46:0)	2.1E+07	1.3E+07	4.6E-03	4.6E-02	1.61	Not
TG	TG57	TG(49:5)	4.1E+06	2.1E+06	4.5E-03	4.6E-02	1.92	Not
PL	PL75	PC(O-36:1)	1.8E+05	3.1E+05	4.9E-03	4.8E-02	0.58	Not

Up, padj<0.05 | Down, padj<0.05

Up, padj<0.05, FC>2 | Down, padj<0.05, FC<0.5

The thesis version of Supplementary Table ST2 does not contain the individual values and the non-significant results, as they do not fit on one page. n=8 per group. Please contact prof Barbara M. Bakker at b.m.bakker01@umcg.nl for the complete table

Supplementary Table ST3. Annotated TG and DG isomers from livers of 8-week-old mice

Name	Isomer1	Isomer2	Isomer3	Isomer4	Isomer5	Isomer6	Isomer7	Isomer8	Isomer9
TG(40:0)	TG(10:0_14:0_16:0)	TG(12:0_12:0_16:0)	TG(12:0_14:0_14:0)	TG(16:0_16:0_8:0)					
TG(40:1)	TG(16:0_16:1_8:0)	TG(14:0_18:1_8:0)	TG(10:0_14:0_16:1)	TG(16:0_18:1_6:0)					
TG(40:2)	TG(10:0_14:1_16:1)	TG(14:0_18:2_8:0)	TG(14:1_18:1_8:0)	TG(16:1_16:1_8:0)	TG(16:0_18:2_6:0)	TG(16:1_18:1_6:0)			
TG(42:0)	TG(10:0_16:0_16:0)	TG(12:0_14:0_16:0)	TG(14:0_14:0_14:0)						
TG(42:1)	TG(10:0_14:0_18:1)	TG(10:0_16:0_16:1)	TG(12:1_14:0_16:0)	TG(16:0_18:1_8:0)					
TG(42:2)	TG(10:0_14:0_18:2)	TG(10:0_16:1_16:1)	TG(12:1_14:1_16:0)	TG(16:0_18:2_8:0)	TG(16:1_18:1_8:0)				
TG(42:3)	TG(10:0_14:0_18:3)	TG(14:1_14:1_14:1)	TG(16:1_18:2_8:0)	TG(16:2_18:1_8:0)	TG(18:1_18:2_6:0)				
TG(43:1)	***TG(9:0_16:0_18:1)***	***TG(10:0_15:0_18:1)***							
TG(44:1)	TG(10:0_16:0_18:1)	TG(12:0_14:0_18:1)	TG(12:0_14:1_18:0)	TG(12:0_16:0_16:1)	TG(12:1_14:0_18:0)	TG(12:1_16:0_16:0)	TG(14:0_14:0_16:1)	TG(14:0_14:1_16:0)	
TG(44:2)	TG(10:0_16:0_18:2)	TG(10:0_16:1_18:1)	TG(12:0_14:0_18:2)	TG(12:0_14:1_18:1)	TG(12:0_16:1_16:1)	TG(12:1_14:0_18:1)	TG(12:1_16:0_16:1)	TG(14:1_14:1_16:0)	TG(18:1_18:1_8:0)
TG(44:3)	TG(10:0_16:0_18:3)	TG(10:0_16:1_18:2)	TG(10:0_16:2_18:1)	TG(12:1_14:0_18:2)	TG(12:1_14:1_18:1)	TG(12:1_16:1_16:1)	TG(18:1_18:2_8:0)		
TG(44:4)	TG(10:0_16:1_18:3)	TG(10:0_16:2_18:2)	TG(12:1_14:1_18:2)	TG(12:1_16:1_16:2)	TG(18:1_18:3_8:0)	TG(18:2_18:2_8:0)			
TG(44:5)	TG(18:2_18:3_8:0)	TG(16:1_20:4_8:0)							
TG(45:1)	TG(12:0_15:0_18:1)	TG(14:0_15:0_16:1)	TG(14:1_15:0_16:0)						
TG(45:2)	TG(12:0_15:0_18:2)								
TG(45:3)	TG(10:1_17:0_18:2)								
TG(46:2)	TG(10:0_18:1_18:1)	TG(12:0_16:0_18:2)	TG(12:0_16:1_18:1)	TG(12:1_16:0_18:1)	TG(12:1_16:1_18:0)	TG(14:0_14:1_18:1)	TG(14:0_16:1_16:1)	TG(14:1_14:1_18:0)	TG(14:1_16:0_16:1)
TG(46:3)	TG(10:0_18:1_18:2)	TG(12:0_16:1_18:2)	TG(12:0_16:2_18:1)	TG(12:1_16:0_18:2)	TG(12:1_16:1_18:1)	TG(14:0_14:1_18:2)	TG(14:1_14:1_18:1)	TG(14:1_16:0_16:2)	TG(14:1_16:1_16:1)
TG(46:4)	TG(10:0_16:0_20:4)	TG(10:0_18:1_18:3)	TG(12:0_16:1_18:3)	TG(12:0_16:2_18:2)	TG(12:1_16:0_18:3)	TG(12:1_16:1_18:2)	TG(12:1_16:2_18:1)	TG(14:1_14:1_18:2)	
TG(46:5)	TG(10:0_18:2_18:3)	TG(12:0_16:2_18:3)	TG(12:1_16:1_18:3)	TG(12:1_16:2_18:2)	TG(16:0_22:5_8:0)	TG(18:1_20:4_8:0)			
TG(46:6)	TG(16:0_22:6_8:0)								
TG(47:4)	no MS/MS								
TG(47:5)	no MS/MS								
TG(47:6)	no MS/MS								
TG(48:4)	TG(12:0_18:2_18:2)	TG(12:1_18:1_18:2)	TG(14:0_16:1_18:3)	TG(14:0_16:2_18:2)	TG(14:1_16:0_18:3)	TG(14:1_16:1_18:2)	TG(14:1_16:2_18:1)	TG(16:0_16:2_16:2)	TG(16:1_16:1_16:2)
TG(48:6)	TG(10:0_16:0_22:6)	TG(10:0_18:2_20:4)	TG(14:1_14:1_20:4)	TG(16:2_16:2_16:2)					
TG(48:7)	TG(10:0_16:1_22:6)								
TG(48:8)	No MS/MS								
TG(50:6)	TG(12:0_16:0_22:6)	TG(12:1_18:1_20:4)	TG(14:0_14:0_22:6)	TG(14:0_18:3_18:3)	TG(14:1_16:1_20:4)	TG(14:1_18:2_18:3)	TG(16:1_16:2_18:3)	TG(16:2_16:2_18:2)	
TG(50:7)	TG(10:0_18:1_22:6)	TG(12:0_16:1_22:6)	TG(12:1_16:0_22:6)	TG(14:1_18:3_18:3)	TG(16:2_16:2_18:3)				
TG(50:8)	low confidence								
TG(60:5)	low confidence								
DG(28:2)	***DG(10:1_18:1)***								

Bold and italic: manually checked. MS1 isomers were combined.

Supplementary Table ST4. Histological examination scores for 16-20-week old and 8-week-old mice

	16-20 weeks-old							8 weeks-old						
	WT			KO				WT			KO			
ORO staining	0.9	±	0.0	0.8	±	0.1	*	0.9	±	0.0	0.8	±	0.1	
ORO Steatosis grade	3.0	±	0.0	2.9	±	0.1		3.0	±	0.0	2.8	±	0.2	
ORO dimension of vesicles	1.4	±	0.2	1.7	±	0.1		2.0	±	0.1	1.8	±	0.2	
Anisokaryosis	0.3	±	0.2	0.3	±	0.3		0.1	±	0.1	0.6	±	0.3	
Steatosis grade	2.8	±	0.2	1.6	±	0.3	*	1.9	±	0.3	2.0	±	0.3	
Location steatosis	2.8	±	0.2	2.1	±	0.1	*	2.1	±	0.1	2.0	±	0.0	
Mircovesicular steatosis	1.0	±	0.0	1.0	±	0.0		1.0	±	0.0	0.9	±	0.1	
Ballooning	0.1	±	0.1	0.0	±	0.0		0.0	±	0.0	0.0	±	0.0	
Lobular inflammation	1.1	±	0.3	1.1	±	0.2		0.8	±	0.3	1.0	±	0.3	
Portal inflammation	0.1	±	0.1	0.3	±	0.2		0.1	±	0.1	0.5	±	0.2	
Pigmented macrophages	0.5	±	0.2	0.1	±	0.1		0.0	±	0.0	0.0	±	0.0	
NAFLD activity score	4.0	±	0.5	2.8	±	0.4	*i*	2.6	±	0.4	3.0	±	0.5	
Ass. Lesions score	1.4	±	0.4	0.5	±	0.5	*i*	0.9	±	0.5	1.0	±	0.7	

Comparisons, statistics and number of mice per group as in Supplementary table ST3.

Supplementary Table ST5. Table of possible lipid fragments

Fatty acyl Searching database

Fatty acid	fa1	fa2	fa3	PL	TG	DG
FA6:0	T	T	T		T	T
FA8:0	T	T	T		T	T
FA9:0	T	T	T		T	T
FA10:0	T	T	T		T	T
FA12:0	T	T	T		T	T
FA12:1	T	T	T		T	T
FA14:0	T	T	T		T	T
FA14:1	T	T	T		T	T
FA15:0	T	T	T		T	T
FA15:1	T	T	T		T	T
FA16:0	T	T	T	T	T	T
FA16:1	T	T	T		T	T
FA16:2	T	T	T		T	T
FA17:0	T	T	T		T	T
FA18:0	T	T	T	T	T	T
FA18:1	T	T	T	T	T	T
FA18:2	T	T	T	T	T	T
FA18:3	T	T	T	T	T	T
FA19:0	T	T	T	T	T	T
FA20:3	T	T	T	T	T	T
FA20:4	T	T	T	T	T	T
FA20:5	T	T	T	T	T	T
FA21:0	T	T	T		T	T
FA22:3	T	T	T		T	T
FA22:4	T	T	T	T	T	T
FA22:5	T	T	T	T	T	T
FA22:6	T	T	T	T	T	
O-16:0	T	T	T	T	T	
O-18:0	T	T	T	T	T	
O-20:0	T	T	T	T	T	
P-16:0	T			T	T	
P-18:0	T			T	T	
P-20:0	T			T	T	

Fragments Score weight

Type	Weight	Group
FA1_[FA-H2O+H]+	1.6	1
FA2_[FA-H2O+H]+	1.6	1
FA3_[FA-H2O+H]+	1.6	1
[MG(FA1)-H2O+H]+	1.6	2
[MG(FA2)-H2O+H]+	1.6	2
[MG(FA3)-H2O+H]+	1.6	2
[M-(FA1)+H]+	30	2
[M-(FA2)+H]+	30	2
[M-(FA3)+H]+	30	2

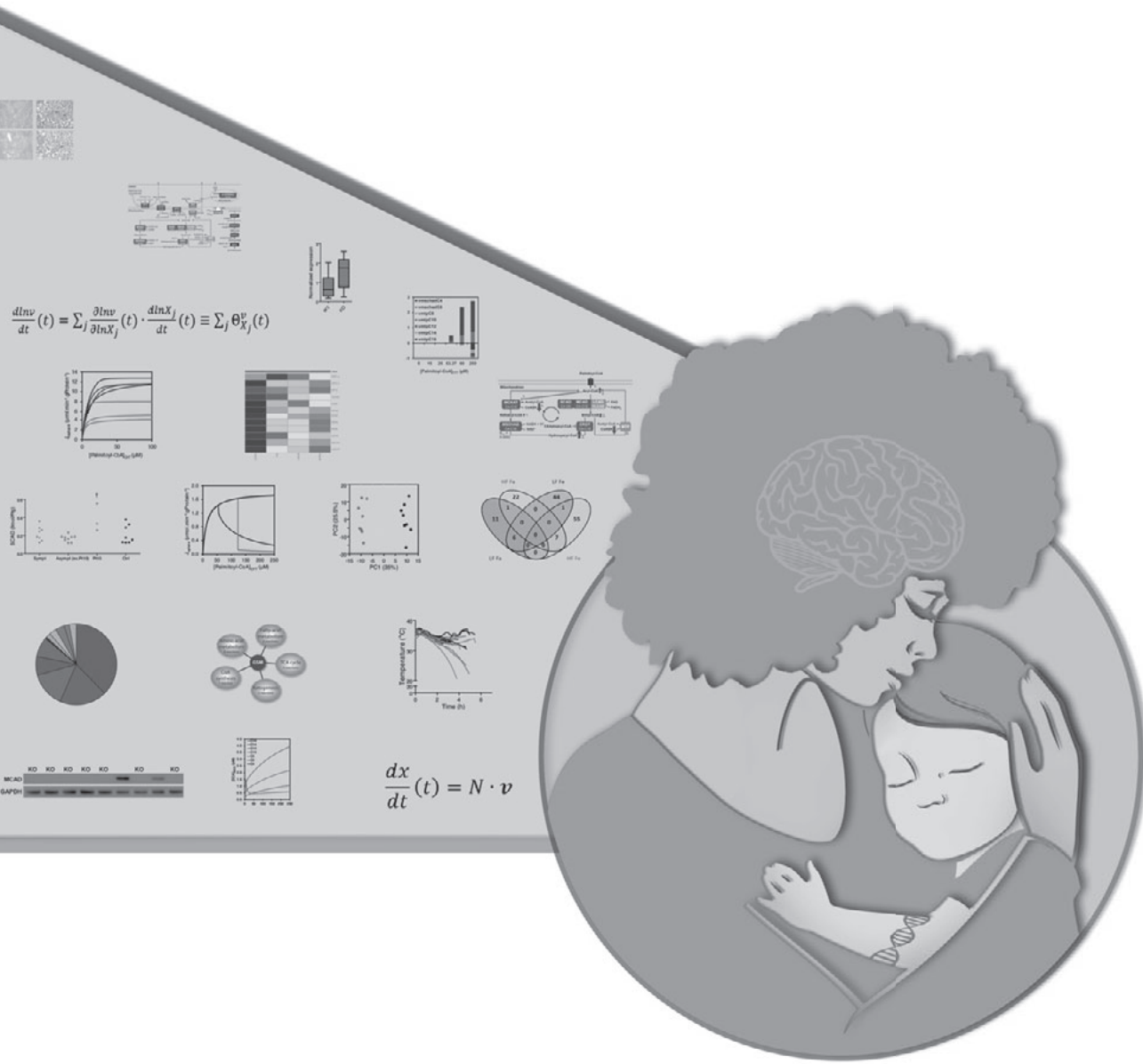
$\frac{dlnv}{dt}(t) = \sum_j \frac{\partial lnv}{\partial lnX_j}(t) \cdot \frac{dlnX_j}{dt}(t) \equiv \sum_j \theta^v_{X_j}(t)$
KO KO KO KO KO KO KO
MCAD
GAPDH
$\frac{dx}{dt}(t) = N \cdot v$